Published in final edited form as:
Biorheology. 2011 January 1; 48(1): 1–35. doi:10.3233/BIR-2011-0579.

Biomechanics of leukocyte rolling

Prithu Sundd[a,*], **Maria K. Pospieszalska**[a], **Luthur Siu-Lun Cheung**[b], **Konstantinos Konstantopoulos**[b], and **Klaus Ley**[a]

[a]Division of Inflammation Biology, La Jolla Institute for Allergy and Immunology, La Jolla, CA, USA.

[b]Department of Chemical and Biomolecular Engineering, Johns Hopkins University, Baltimore, MD, USA.

Abstract

Leukocyte rolling on endothelial cells and other P-selectin substrates is mediated by P-selectin binding to P-selectin glycoprotein ligand-1 expressed on the tips of leukocyte microvilli. Leukocyte rolling is a result of rapid, yet balanced formation and dissociation of selectin-ligand bonds in the presence of hydrodynamic shear forces. The hydrodynamic forces acting on the bonds may either increase (catch bonds) or decrease (slip-bonds) their lifetimes. The force-dependent 'catch-slip' bond kinetics are explained using the 'two pathway model' for bond dissociation. Both the 'sliding-rebinding' and the 'allosteric' mechanisms attribute 'catch-slip' bond behavior to the force-induced conformational changes in the lectin-EGF domain hinge of selectins. Below a threshold shear stress, selectins cannot mediate rolling. This 'shear-threshold' phenomenon is a consequence of shear-enhanced tethering and catch-bond enhanced rolling. Quantitative dynamic footprinting microscopy has revealed that leukocytes rolling at venular shear stresses (> 0.6 Pa) undergo cellular deformation (large footprint) and form long tethers. The hydrodynamic shear force and torque acting on the rolling cell are thought to be synergistically balanced by the forces acting on tethers and stressed microvilli, however, their relative contribution remains to be determined. Thus, improvement beyond the current understanding requires *in silico* models that can predict both cellular and microvillus deformation and experiments that allow measurement of forces acting on individual microvilli and tethers.

Keywords

Quantitative dynamic footprinting (qDF); footprint; P-selectin; event tracking model of adhesion (ETMA); immersed boundary method (IBM)

1. Introduction

Inflammation is an acute response coordinated by the innate arm of the immune system and involves leukocyte recruitment from the blood stream into the inflamed tissue [100,112,134,147,149,176,187]. Although the first set of observations of leukocyte recruitment across the blood-tissue barrier date back to the early nineteenth century [1,38,203-204,207], the studies done over the last two decades [7,10,11,53,76,77,95,96,105,111,118,191,201,223] have inspired the creation of a paradigm for the leukocyte recruitment to the inflammatory foci [112,147]. Neutrophil, or polymorphonuclear (PMN) leukocytes, are the most abundant leukocytes in the peripheral

* Address for correspondence: Dr. Prithu Sundd, Division of Inflammation Biology, La Jolla Institute for Allergy and Immunology, 9420 Athena Circle Drive, La Jolla, CA 92037, USA. Tel: +1 858752-6702; Fax: +1 858 752-6985; prithu@liai.org.

blood of humans and are recruited to the site of acute inflammation [3]. The neutrophil recruitment takes place primarily in the postcapillary venules of the inflamed tissue and involves neutrophil adhesion to the vessel endothelium against the hemodynamic shear forces exerted by the flowing blood [10,11,95]. Neutrophil adhesion to the vessel endothelium requires coordination of several steps, each dependent on non-covalent interactions of specific adhesion receptors (AR) on the neutrophil or endothelium with their respective ligands on the apposing cell [21,112,187]. Rolling initiates with the first step of capture which can result in rolling along the vessel endothelium followed by slow rolling, activation, and firm arrest [112]. Collision with red blood cells (RBC) and RBC aggregates cause neutrophils to marginate towards the blood vessel wall [55,137,164]. The free flowing marginated neutrophils tether and roll along the vessel endothelium through reversible and rapid interactions between the selectin family of adhesion molecules expressed on (P, E-selectin) endothelial cells (EC) or neutrophils (L-selectin) with their carbohydrate ligands expressed on the apposing cell to mediate the primary steps of capturing and rolling [33,36,49,126,196]. Neutrophil rolling in the postcapillary venules is predominantly mediated by P-selectin expressed on the EC binding to its sialo-mucin ligand P-selectin glycoprotein ligand (PSGL)-1 constitutively expressed on the neutrophils [20,76,87,96,111,133,138-139]. Neutrophil rolling along the vascular endothelium of the cremaster or mesenteric postcapillary venules has been studied extensively using *in vivo* intravital microscopy [10,11,32,33,49,75-77,96,111,149,182].

Flow chamber assays have proved to be an excellent model to replicate the selectin-mediated rolling of neutrophils in an *in vitro* setting [7,53,102,103,105,142,155,162,166,180,191]. Neutrophils in a physiological buffer or whole blood are allowed to flow in laminar flow regime (Reynolds number, R_e <<1) over a glass or polystyrene substrate either coated with EC, recombinant or purified selectins or selectin ligands. The hydrodynamic forces experienced by the rolling cells are estimated from the shear stress exerted by the streaming fluid on the flow chamber wall [54,92] and the volumetric flow rates are adjusted to achieve venular wall shear stresses (0.12 to 3.5 Pa) [33]. These *in vivo* and *in vitro* studies have profoundly contributed to the current understanding of the biomechanics of neutrophil rolling on selectin substrates.

The measurements of cellular and molecular biophysical parameters generated in these studies have inspired the creation of several *in silico* theoretical models [22,23,26,36,37,60,72,84,85,88, 93,145,150,152,196,226] which are capable of simulating neutrophil rolling at temporal resolutions 10-10^4 times higher than those possible experimentally. These models predict that the phenomenon of rolling is a result of balanced but rapid formation and dissociation of selectin-carbohydrate bonds at the front and rear of the rolling cell, respectively, under the influence of shear forces exerted by the streaming media. This molecular mechanism responsible for neutrophil rolling, which was introduced two decades ago, [35,60,196] has also been observed experimentally [191]. Quantitative dynamic footprinting (qDF) microscopy revealed that the selectin-carbohydrate bonds in the footprints of rolling neutrophils are relaxed in the front where they form, compressed in the center, and stressed at the rear of the footprint where they finally break away from the substrate [191]. The same study also revealed that the footprint of a neutrophil rolling at high wall shear stress (> 0.6 Pa) is four times larger than that reported by the *in vivo* studies as well as theoretical models and that rolling neutrophils also form three to four long tethers at the rear which can extend up to 16 μm behind the cell footprint [191]. In addition to verifying the molecular mechanism of rolling predicted by theoretical models, these findings also provide an insight into the discrepancy between the rolling behavior predicted theoretically and that observed experimentally. Stable neutrophil rolling is observed in venules *in vivo* [33] and in whole blood flow chambers *in vitro* [31,98,191] at shear stresses higher than 0.6 Pa. However, theoretical models predict rolling only at small shear stresses

(< 0.2 Pa) and fail to reproduce stable rolling at high shear stresses (> 0.6 Pa) commonly observed *in vivo* [88,150]. Neutrophils are deformable cells and their surface is covered with interconnected ridges of microvilli which are membrane structures ~200 nm long [48,163]. With increasing wall shear stress, rolling neutrophils deform thus creating a larger footprint [33,49,191], the microvilli undergo extension, and may form tethers [142,155,166,191]. In tether formation, the cytoskeleton is separated from the plasma membrane [209,210]. None of the currently available theoretical models [72,85,88,150] take all three biophysical phenomena into consideration. This may limit the ability to model rolling of neutrophils at high shear stress. This review provides an overview of the current understanding of the biomechanics of neutrophil rolling on selectin substrates.

2. Adhesion molecules

2.1. Selectins

Neutrophil rolling in postcapillary venules *in vivo* [76,87,111] and flow chambers *in vitro* [53,102,104-105,129, 205] is mediated by the selectin family of adhesion molecules, P-, E-, and L-selectin. Models of gene-deficient mice have revealed that deletion of a single selectin leads to moderate [8,99,125,190,194] while deletion of more than one leads to severe inflammatory disorders [18,19,50]. Selectins are type I transmembrane glycoproteins that share a common structural organization across all mammalian species [80,185,193,200]. The N-terminus of each selectin has a Ca^{2+}-dependent carbohydrate recognition domain which is characteristic of C-type lectins, followed by an epidermal growth factor (EGF) like domain, a series of short consensus repeats which vary in number among the three selectins within species as well as for the same selectin within different species [127,128,200]. The number of consensus repeats determines the length of the extracellular domain of each selectin. Selectins also have a transmembrane domain followed by a short cytoplasmic domain. The length of extracellular domains, expression levels, molecular density, role in leukocyte rolling, and physiological ligands for different selectins are shown in Table 1.

2.1.1. P-selectin—P-selectin mediates neutrophil rolling in the postcapillary venules of mice *in vivo* [87,96,111] and flow chambers *in vitro* [20,105,205]. It also mediates interactions of activated platelets with neutrophils [225] and monocytes [119]. Although P-selectin is undetectable on the surface of EC of most tissues of mice *in vivo* and cultured EC *in vitro* under baseline conditions [64,75], it is stored preformed in the Weibel-Palade bodies of EC and is rapidly translocated to the plasma membrane following stimulation with histamine or thrombin *in vitro* [52,64] or surgery-induced trauma *in vivo* [41,75,87]. Cultured human umbilical vein EC (HUVEC) are known to express P-selectin at a site density of 20-50 molecules/μm^2 within 5-10 min following treatment with histamine [64]. In addition, P-selectin transcription and translation are upregulated in EC within 2 h following cytokine treatment [41,57,59,75,160,211]. P-selectin is an extended molecule with an extracellular domain that varies in length among different species based on the number of consensus repeats present [200]. The extracellular domain of human P-selectin has nine short consensus repeats and is 38 nm long (refer Table 1) [199]. However, the mouse P-selectin has eight short consensus repeats and is 34 nm long [199-200]. P-selectin expressed on EC forms homodimers through noncovalent interactions of its transmembrane domains [14,199]. P-selectin clustering on EC through interaction of its cytoplasmic tails with clathrin-coated pits has been shown to enhance neutrophil rolling [168,170]. *In vivo* studies using gene-deficient mice and function blocking antibodies have revealed that neutrophil rolling along the vascular endothelium of postcapillary venules during the first one hour following surgery-induced trauma or cytokine induced inflammation is predominantly mediated by endothelial expressed P-selectin with an average rolling velocity of 40 μm/s [33,74,76,96,111]. Rolling of human neutrophils on different site densities of P-selectin has

been studied *in vitro* as a function of wall shear stress [105] and the data from this study is shown in Fig. 1.

2.1.2. E-selectin—E-selectin expression is restricted to EC and is undetectable in most tissues under baseline conditions but gets upregulated within 2 h following cytokine treatment [41,75]. Cultured human microvascular EC (HMVEC) have been shown to express E-selectin at a site density of 750 molecules/μm^2 following 5 h treatment with interleukin (IL)-1α [110]. E-selectin mediates slow rolling of neutrophils on cytokine activated EC *in vivo* [76,182] and immobilized E-selectin *in vitro* [101,104,179]. The slow rolling of neutrophils (rolling velocity ≤ 5 μm/s) following tumor necrosis factor (TNF)-α induced inflammation is absent in mice deficient in E-selectin, and this is reproduced in wild type mice treated with anti-E-selectin mAb [97]. E-selectin dependent slow leukocyte rolling requires the β_2 integrin LFA-1 [223]. The extracellular domain of human and mouse E-selectin contains one lectin domain, one EGF domain, and six short consensus repeats and extends 27 nm above the plasma membrane (refer Table 1) [199,200]. E-selectin expressed on EC colocalizes as clusters in membrane rafts and clathrin-coated pits and this clustering has been shown to stabilize neutrophil rolling [169].

2.1.3. L-selectin—L-selectin is constitutively expressed on neutrophils, monocytes, and lymphocytes [80,185] and rapidly shed from the cell surface following cellular activation by chemoattractants and activating factors, which involves proteolytic cleavage at a membrane proximal site [58,78,89]. L-selectin monomers are clustered on the tips of neutrophil microvilli (30,000-40,000 molecules per human neutrophil [177]) which facilitates capturing of free flowing neutrophils by presentation of L-selectin to EC-bound ligands [44,48,101,202]. L-selectin is the smallest of the three selectins with an extracellular domain that contains only two short consensus repeats in addition to the lectin and EGF domains and extends ~12 nm from the plasma membrane in both mice and humans (refer Table 1) [199,200]. Studies using gene deficient mice and function-blocking antibodies have shown that L-selectin mediates fast rolling (rolling velocity > 100 μm/s [74]) of neutrophils in inflamed as well as noninflamed peripheral post capillary venules [8,76,97,111,113-114]. However, studies done with mice *in vivo* [43,94,182] and flow chambers *in vitro* [13,205] have also shown that most of the L-selectin mediated fast rolling of neutrophils is a result of secondary capture or tethering of free flowing neutrophils by adhered or rolling neutrophils.

2.2. PSGL-1 and other selectin ligands

P-selectin glycoprotein ligand-1 (PSGL-1) constitutively expressed on neutrophils is a ligand for all three selectins (P-, E-, L-selectin) and mediates neutrophil rolling in the peripheral microvasculature *in vivo* [42,67,138,182-183,214,222] and flow chambers *in vitro* [31,98,124,205,214]. PSGL-1 is the dominant ligand on neutrophils to mediate P-selectin dependent rolling both *in vivo* [138-139,183] and *in vitro* [105,133,144,156,191]. PSGL-1 also serves as a ligand for L-selectin during secondary capture of neutrophils by already adhered neutrophils both *in vivo* and *in vitro* [6,42,43,79,94,117,143,182,184,188,197,205]. PSGL-1 is a transmembrane disulfide-linked homodimeric sialo-mucin constitutively expressed on the tips of microvilli at a site density of 75,000 molecules per mouse neutrophil, 18,000-25,000 molecules per human neutrophil, and 36,000 molecules per HL-60 cell [24,127,129,133,138,185,199,200, 224]. The localization of PSGL-1 on the microvilli tips has been shown to enhance P-selectin-PSGL-1 mediated tethering by increasing the probability of interactions between the two molecules [115,133,218]. PSGL-1 is an extended molecule with an extracellular domain which extends out ~50 nm above the plasma membrane and consists of decameric repeats rich in threonine, serine, and proline [2,12,115,159,192]. Threonine and serine residues throughout the extracellular domain of PSGL-1 are glycosylated to bear sialylated, fucosylated O-glycans capped with the sialyl

Lewis-x or sLe^x [NeuAcα2–3Galβ1–4(Fucα1–3)GlcNAcβ1-R] tetrasaccharide determinant [127-129,132,187,200]. P- and L-selectin binding to PSGL-1 is the result of interactions of lectin domain residues and the Ca^{2+} ion in the lectin domain with the sLe^x determinant on short core 2 O-glycan expressed on the N-terminal threonine (Thr17 in mice and Thr57 in humans), adjacent to sulfated tyrosine residues (Tyr13 in mice and Tyr46, Tyr48, and Tyr51 in humans) [24,40,107-109,120,153,181,213]. E-selectin binding to PSGL-1 does not require sulfated tyrosine residues and is mediated by the lectin domain and Ca^{2+} ion interacting with the sLe^x determinant expressed on core 2-O glycans throughout the PSGL-1 ectodomain [116,181]. Uncharacterized L-selectin ligands expressed on EC of postcapillary venules of mouse cremaster also mediate neutrophil rolling *in vivo* [174].

L-selectin also binds to a family of sialylated, fucosylated, and sulfated mucins known as peripheral node addressins (PNAds) expressed in high endothelial venules [129,157]. PNAd is defined by its reactivity with MECA-79, a mAb that recognizes 6-sulfo-*N*-acetylglucosamine (GlcNAc-6-sulfate) [66,157]. The protein composition of PNAd includes glycosylated cell adhesion molecule-1 (GlyCAM-1), CD34, and podocalyxin. PNAd mediates L-selectin dependent rolling of lymphocytes in high endothelial venules of lymph nodes by presenting a sulfated form of sLe^x on extended core 1 O-, branched core 2 O-, and N-glycans expressed throughout the ectodomain [83,129,131,157,198]. In addition to PSGL-1, E-selectin mediated rolling of neutrophils in the peripheral microvasculature of mice is also mediated by N-glycans on E-selectin ligand-1 (ESL-1) and CD44 expressed on murine neutrophils [67,82,106]. ESL-1 is localized on microvilli but away from the tips [189] and has been shown to synergize with PSGL-1 to mediate initial tethering on E-selectin and with CD44 localized on the cell body [202] to mediate slow-steady rolling [67]. Recently, core 2 O- and extended core 1 O-glycans on uncharacterized glycoproteins other than PSGL-1, ESL-1, and CD44 expressed on mouse neutrophils have also been proposed to mediate tethering and rolling on E-selectin both *in vivo* and *in vitro* [217]. Human neutrophils have been shown to express sialylated glycosphingolipids which mediate E-selectin dependent tethering and rolling *in vitro* [136].

3. Forces acting on a rolling neutrophil

Rolling is a characteristic ‘jerky-tumbling’ motion of neutrophils along the blood vessel wall *in vivo* and selectin substrate *in vitro* in the presence of hydrodynamic shear flow [11,28,105]. Shear flow exerts a hydrodynamic shear force F_s (in the *x* direction), and torque T_s (in the *y* direction about the cell center), on a neutrophil adhered to a P-selectin coated substrate [60,196] (Fig. 2). Neutrophils interact with a P-selectin substrate through noncovalent bonds between PSGL-1 expressed on the microvilli tips and P-selectin on the substrate [15,133]. As the adhered neutrophil under shear flow moves forward, the hydrodynamic shear force and torque is translated into force on the bonds at the rear of the neutrophil [35,60,129,196]. The force acting on the bonds increases with the forward motion of the cell until it balances the hydrodynamic shear force and torque, causing the cell to stop. Eventually, the stressed bonds at the rear fail, allowing the cell to undergo a jerky rolling motion in the direction of flow. As the cell rolls forward, it forms new bonds in the front, while the unloaded bonds, which were earlier in the center of the cell footprint, are now exposed at the rear and start to bear stress, causing the cell to retard. Since PSGL-1 is clustered on the tips of microvilli, the force acting on all bonds on a microvillus can be collectively summed up as the force acting on the microvillus, F_{mv}, causing it to stretch [150,152]. Neutrophils rolling at high shear stress are known to form long membrane tethers (discussed in section 4.2.3) at the rear of the cell and these tethers have been suggested to contribute synergistically with the stressed microvilli to balance the hydrodynamic shear force and torque [142,155,166,191]. Recently, qDF microscopy revealed that neutrophils rolling at high shear stress ($\tau_w \geq 0.6$ Pa) form 3-4 long tethers behind the cell footprint and

these tethers synergize with less than 10 stretched microvilli in the rear portion of the cell footprint to stabilize rolling [191].

A schematic of a neutrophil rolling on P-selectin coated substrate under a shear flow ($\tau_w \geq 0.6$ Pa) is shown in Fig. 2. As the Reynolds number is very much less than unity, the inertial forces are negligible [54,63]. The shear force F_s and torque T_s acting on a stationary sphere close to the wall in a semi-infinite linear shear flow are calculated from Goldman et al.'s expressions [54] shown in Eqs. 1 and 2, assuming a cell body to substrate separation distance of 25 nm [191]:

$$F_s = 31.97 \tau_w r_c^2 \tag{1}$$

$$T_s = 11.87 \tau_w r_c^2 \tag{2}$$

where τ_w is the wall shear stress and r_c is cell radius. A force balance on the rolling neutrophil along the x and y-axis results in Eqs. 3 and 4:

$$F_s = \sum_{i=1}^{n} F_{te,i} \cos\varphi_i + \sum_{j=1}^{m} F_{mv,j} \cos\theta_j \tag{3}$$

$$F_N = \sum_{i=1}^{n} F_{te,i} \sin\varphi_i + \sum_{j=1}^{m} F_{mv,j} \sin\theta_j \tag{4}$$

where F_N is the normal reaction force, $F_{te,i}$ is the force on the i^{th} tether, $F_{mv,j}$ is the force on the j^{th} stressed microvillus (the symbol is used to denote the force when there is no tether), and φ_i and θ_i are the corresponding angles as shown in Fig. 2. The torque in the y direction about the cell center due to $F_{te,i}$ is denoted by T_{tei}, and due to $F_{mv,j}$ by $T_{mv,j}$. A moment balance about the center of the rolling neutrophil results in Eq. 5:

$$T_s = \sum_{i=1}^{n} T_{te,i} + \sum_{j=1}^{m} T_{mv,j} \tag{5}$$

The angles φ_i and θ_j can be calculated from L_i and l_j, respectively. The solution for the forces acting on the individual tethers and stressed microvilli and the torques generated by these forces requires the knowledge of their relative contribution in counterbalancing the hydrodynamic drag.

4. Biomechanics of selectin-mediated rolling

4.1. Molecular biomechanics

As discussed in the previous section, hydrodynamic shear forces acting on the rolling neutrophils are translated into molecular forces of disruption that stretch the P-selectin-PSGL-1 bonds at the rear of the rolling neutrophil [35,60,196]. Stretched P-selectin-PSGL-1 bonds behave like Hookean springs and the force F_b acting on a stretched bond is a linear function of the strain in the direction of the force as shown in Eq. 6 [22,34,35,152]:

$$F_b = \sigma\left(L_{sep} - \lambda\right) \tag{6}$$

where L_{sep} and λ are the stressed and unstressed length of the P-selectin-PSGL-1 molecular complex, respectively and σ is the bound state spring constant of the complex. $F_b = 0$, if $L_{sep} \leq \lambda$. Thus, neutrophil rolling on a P-selectin substrate in the presence of hydrodynamic shear flow is a consequence of the temporal balance between the hydrodynamic and Hookean forces and the torques generated by them. The strain in P-selectin-PSGL-1 bonds in response to tensile forces in the range that are generated during rolling of neutrophils under physiological conditions has been measured using atomic force microscopy [51]. The P-selectin-PSGL-1 bonds were shown to withstand tensile forces up to 165 pN and extend up to 125 nm [51]. Molecular strain measurements in response to piconewton forces in live rolling neutrophils were made by qDF microscopy [191]. qDF micrographs were used to generate 3D footprints of rolling neutrophils (representative example shown in Fig. 3) which show the *x*- and *z*-coordinates of individual microvilli tips in the footprint. These 3D footprints (Fig. 3) revealed that the P-selectin-PSGL-1 bonds are unstressed ($L_{sep} = \lambda = 70$ nm [144,150,152]) in the front where they form, compressed in the center ($L_{sep} < 70$ nm), and stressed beyond the equilibrium length ($L_{sep} > 70$ nm) at the rear of the footprint where they finally fail. An average maximum strain, L_{sep}(max), of 133 nm was measured for P-selectin-PSGL-1 bonds at the rear of the footprint, which is 190% of the unstressed length, λ, of the P-selectin-PSGL-1 molecular complex. Based on Eq. 6, these results experimentally validate that the molecular bonds only at the rear and not in the front or center of the footprint of a rolling neutrophil are under tensile stress.

Neutrophil rolling requires rapid formation of new bonds in the front and rapid dissociation of stressed bonds at the rear under the influence of shear forces [35,60,196]. The forces acting on the bonds can regulate the dynamics of neutrophil rolling by facilitating or retarding the dissociation of the stressed bonds at the rear. The selectin-carbohydrate molecular interaction is reversible and regulated by the chemical kinetics of the bond formation and dissociation as shown in Eq. 7 [15,35]:

$$\mathrm{R+L} \underset{k_r}{\overset{k_f}{\rightleftarrows}} \mathrm{RL} \tag{7}$$

where R is the receptor (P-selectin), L is the ligand (PSGL-1), RL is the receptor-ligand (P-selectin-PSGL-1) molecular complex, and k_f and k_r are the forward and reverse reaction rates, respectively. The reverse reaction follows first order chemical kinetics, but the lifetime of the selectin-carbohydrate bond ($1/k_r$) is also modulated by the force acting on the bond. Depending on the bond force, selectin-carbohydrate bonds may behave as ‘catch bonds’ for which the life time increases, or ‘slip bonds’, for which the lifetime decreases with increasing bond force [34,35,123]. These bonds have been shown to regulate neutrophil rolling under physiological wall shear stresses [27,123,129,143,219].

4.1.1. Slip bond kinetics—Neutrophil rolling on P-selectin substrates at venular wall shear stresses ($\tau_w > 0.12$ Pa) [33] *in vitro* is predominantly mediated by slip bonds [123]. Slip bonds exhibit the intuitive behavior of decreasing their lifetime in response to increasing bond forces [34-35,123]. The bond force is expected to reduce the free energy barrier between the bound and free states, thereby promoting receptor-ligand bond dissociation [15,35,47]. However, the optimal force above which different selectin-carbohydrate bonds behave like slip bonds differ between P- and L-selectin [129]. The P-selectin-PSGL-1 bonds that mediate neutrophil rolling in *in vitro* flow chambers behave as

slip bonds at wall shear stresses in excess of 0.02 Pa, which corresponds to a force of at least 20 pN per bond [123]. In contrast, L-selectin-PSGL-1 bonds that mediate secondary capture of neutrophils *in vitro* [13,143,205] behave as slip bonds at wall shear stresses in excess of 0.1 Pa, which corresponds to a bond force of at least 100 pN [129,219,228]. The dissimilarity in the slip bond behavior exhibited by different selectins binding to the same ligand is a result of the difference in intrinsic kinetics of bond formation and dissociation which is a consequence of differences in their molecular structure and tensile force-induced conformational change in lectin-EGF domain interface (discussed in section 4.1.2) [121,122,129,186]. Over the last two decades, several *in vitro* studies have experimentally validated the kinetics of slip-bond assisted neutrophil rolling on P-selectin substrates [7,27,156,179]. These experiments involved tethering and rolling of isolated neutrophils on very low densities of immobilized P-selectin at venular wall shear stresses, conditions which favor unimolecular interactions between neutrophil and P-selectin substrate. In these experiments, the lifetime of transient tethers were measured at different wall shear stresses and the rate of detachment of the tethered neutrophils from the substrate was used as an estimate for the rate of P-selectin-PSGL-1 bond dissociation. The experimental data was matched with a theoretical model of receptor-ligand interaction in the presence of tensile force, and the reverse reaction rate was extracted as a function of bond force. Two theoretical models that have been widely used over the last two decades to describe the force dependence of slip bond dissociation kinetics are the model for specific adhesion of cells to cells proposed by Bell (1978) [15] and the Hookean spring model for adhesion of a membrane to surface proposed by Dembo (1988) [35]. Within the ranges of forces and distances found during rolling, the two models yield nearly identical results (Pospieszalska and Ley, unpublished data).

Bell model: The Bell model [15] states that the lifetime of a receptor-ligand bond decreases exponentially with increasing tensile force; therefore, a receptor-ligand bond subjected to tensile force behaves as a ‘slip’ bond. The forward and reverse reactions are shown in Eq. 7 and the tensile force acting on a bond is shown in Eq. 6. The dependence of the reverse reaction rate, k_r, on the tensile force F_b acting on the bond is defined by:

$$k_r = k_r^o \exp\left[\frac{\gamma F_b}{\kappa_B \mathrm{T}}\right] \tag{8}$$

where k_r^o is the unstressed reverse reaction rate at zero force ($F_b = 0$) and γ is the reactive compliance with units of length. The reactive compliance describes the susceptibility of the bond to fail under tensile force. Large γ implies a more compliant bond. κ_B is Boltzmann's constant and T is the absolute temperature. Based on the Boltzmann distribution at equilibrium, the forward reaction rate, k_f, was proposed to be dependent on the separation distance, L_{new}, between the bases of the receptor and the ligand [22] as shown in Eq. 9:

$$k_f = k_f^o \exp\left[\frac{\sigma\,|L_{new} - \lambda|\,(\gamma - \frac{1}{2}\,|L_{new} - \lambda|)}{\kappa_B \mathrm{T}}\right] \tag{9}$$

Where L_{new} is the length of the new bond, λ is the equilibrium unstressed length of the receptor-ligand bond, k_f^o is the unstressed forward reaction rate which is defined as the forward rate when the new bond is of the same length as the equilibrium bond length, i.e. $L_{new} = \lambda$. Several *in vitro* flow chamber studies have validated that the force dependence of the selectin-ligand reverse reaction rate follows Bell model in the force regime that favors slip bonds [5,7,28,156,179].

Dembo model: The model proposed by Dembo et. al. (1988) [35] is based on the assumption that the unstressed transition state and the bound state of the receptor-ligand complex only differ in their spring constants, and the equilibrium constant for the formation of the stretched bond can be defined as:

$$\frac{k_f}{k_r}=\exp\left[\frac{-\sigma_{ts}\left(L_{sep}-\lambda\right)^2}{2\kappa_B T}\right] \tag{10}$$

where k_f and k_r are forward and reverse reaction rate, respectively; k_f^o and k_r^o are the unstressed forward and reverse reaction rate, respectively, σ is the bound state spring constant, L_{sep} is the stretched length of the bond, λ is the equilibrium length of the bond, κ_B is the Boltzmann's constant, and T is the absolute temperature. The forward reaction rate is defined as:

$$k_f=k_f^o\exp\left[\frac{-\sigma_{ts}\left(L_{sep}-\lambda\right)^2}{2\kappa_B T}\right] \tag{11}$$

where σ_{ts} is the transition state spring constant. Substitution of Eq. 11 in Eq. 10 results in the reverse reaction rate, k_r, shown in Eq. 12:

$$k_r=k_f^o\exp\left[\frac{(\sigma-\sigma_{ts})\left(L_{sep}-\lambda\right)^2}{2\kappa_B T}\right] \tag{12}$$

Bonds behave as ‘slip’ bonds for $\sigma > \sigma_{ts}$ and ‘catch’ bonds (discussed in section 4.1.2) if $\sigma < \sigma_{ts}$. The problem with the Bell and Dembo models is that γ and σ_{ts} cannot be measured experimentally. Therefore, estimates based on curve fitting are widely used [4-5,7,39,123,156,179].

The symbols used for biophysical parameters are defined in Table 2. The values of k_f^o and k_r^o for different selectin-ligand pairs have been measured experimentally using *in vitro* rolling assays [5,7,27,156,179], surface plasmon resonance [90,130,135], atomic force microscopy [61,62,123], and micropipette manipulation [195]. Values of these parameters are shown in Table 3. Although the Bell and Dembo models predict the force dependence of slip bond dissociation kinetics, they are not suitable for validating the catch-slip bond transitional behavior exhibited by selectin-ligand bonds from small to large forces. The two pathway model (discussed in section 4.1.2) proposed by Evans and coworkers (2004) is currently the most widely used model to study the catch-slip bond transition [46].

4.1.2. Catch bond kinetics and shear threshold phenomenon—As a theoretical possibility, Dembo and coworkers (1988) suggested that the lifetime of a receptor-ligand bond may decrease, increase or remain unchanged upon application of an external force; these bonds were referred to as ‘slip’, ‘catch’ and ‘ideal’ bonds, respectively [35]. The first experimental demonstration of the counter-intuitive phenomenon in which P-selectinligand bonds resist breakage and become stronger under the influence of a “low” external force was made in 2003 [123]. Application of higher forces dissociates the P-selectin-PSGL-1 bond via the slip dissociation pathway (discussed in section 4.1.1). To date, the catch-to-slip bond transition under progressively increasing forces has been demonstrated experimentally for P-

selectin-PSGL-1 [46,123] and L-selectin binding to PSGL-1 and endoglycan [161]. It is noteworthy that the L-selectin-PSGL-1 bond strengthening due to the catch bond behavior, as quantified by the decrease in k_r relative to the unstressed reverse reaction rate constant, k_r^o, is more pronounced than that of P-selectin-PSGL-1 bond (5-fold versus 2-fold decrease) [123,161]. Moreover, this catch bond behavior is detected over a wider range of external forces for L-selectin (up to 50 pN per bond) relative to P-selectin (up to 20 pN per bond) [123,161].

Evans and colleagues (2004) proposed a two-pathway model to describe the catch-slip bond behavior [46]. The two pathways for bond dissociation originate from two possible bound state configurations. Pathway 1, which occurs with a bond dissociation rate k_{1rup}, is very fast and dominates at low forces, whereas pathway 2 with a bond dissociation rate k_{2rup} is slower and dominates in the high shear regime. It is assumed that k_{1rup} for the fast pathway is constant [46]. For the slow pathway, bond dissociation follows the Bell model (Eq. 8), and can be defined as $k_{2rup}=k_2^0 \exp(\gamma F_b/\kappa_B T)$, where k_2^0 is the unstressed reverse reaction rate for that pathway and F_b is the force on the bond (Eq. 2) [15]. The selectin-ligand bond dissociates along the dominant pathway, which is determined by the occupancy ratio of the two states (S_1/S_2). Under the application of force, the energy of each state shifts to cause a change in the occupancy ratio of the two bound states as shown in Eqs. 13 and 14 [46]:

$$\frac{S_1}{S_2}=\Phi_o \exp\left[-\frac{F_b}{f_{12}}\right] \tag{13}$$

$$\Phi_o=\exp\left[\frac{\Delta E_{21}}{\kappa_B T}\right] \tag{14}$$

where Φ_0 is the initial occupancy ratio under static conditions, f_{12} is the force scale at which the occupancy ratio (S_1/S_2) changes 2.7-fold, and ΔE_{21} represents the difference in energy between the two states which is about 4 - 5κ_BT for P-selectin-PSGL-1 binding [46]. The switch from the low impedance pathway 1 to the high impedance pathway 2 by the application of force is governed by the change in the occupancies of the two bound states, and this determines the transition from catch to slip bond behavior. For bonds exhibiting catch-slip transition, the overall bond dissociation rate can be defined as shown in Eq. 15 [46]:

$$k_r=\frac{\Phi_o k_{1rup}+\exp\left(\frac{F_b}{f_{12}}\right)\left[k_2^o \exp\left(\frac{\gamma F_b}{\kappa_B T}\right)\right]}{\Phi_o+\exp\left(\frac{F_b}{f_{12}}\right)} \tag{15}$$

Based on the crystal structure and molecular dynamics simulations of L- or P-selectin bound to sLe^x or PSGL-1-derived glycosulfopeptide, site-directed mutagenesis, Monte Carlo modeling, and flow chamber assays [90-91,121,129,148,181], two models, the ‘sliding-rebinding mechanism’ [121,122,129] and the ‘allosteric model’ [186,206], have been proposed to relate ‘catch-slip’ bond behavior to the tertiary structure of lectin-EGF domains of selectins. The ‘sliding-rebinding’ model emphasizes the angle between the lectin domain and the EGF-like domain of the selectin molecule [121,122]. Molecular dynamics simulations revealed that the structure of P-selectin bound to PSGL-1 has an interdomain angle of 139.3°, which corresponds to the open-angle or extended conformation, whereas that of P-selectin bound to sLe^x has an interdomain angle of 114.6° which corresponds to the

closed-angle or bent conformation [122]. When tensile force is applied to the selectin-ligand complex, there is a greater probability for the selectin to exist in the open angle or extended conformation [121]. Taking into account the noncovalent interactions at the atomic level, molecular dynamics simulations of P-selectin unbinding from PSGL-1 showed that the interdomain angle opening allows rotation of the lectin domain, tilts the binding interface and aligns it with the direction of force [122]. This is thought to result in sliding of the ligand along the binding interface causing the preexisting interactions to dissociate and allowing new interactions between the two sides of the interface, thereby bringing the system back to its previously bound state. This prolongs the lifetimes by slowing dissociation, resulting in catch bonds. The PSGL-1 glycan: fucose, sialic acid, galactose, N-acetylglucosamine and eight residues from the PSGL-1 peptide including three sulfated tyrosines were observed to form new interactions most frequently [122]. Once the interdomain angle is fully open, the probability for rebinding becomes maximum. Further increase in applied force will not increase the lifetimes, but rather accelerate the dissociation resulting in the catch-to-slip bond transition [122].

The ‘allosteric model’ was introduced by Waldron and Springer (2009) based on the crystal structures of P-selectin in the absence or presence of ligand [206]. Waldron and Springer (2009) identified a lobe in the lectin domain that reorients upon ligand binding [206]. Reorientation of this lobe induces the movement of a loop (residues 83-89), which approaches the ligand binding site, thereby augmenting the ligand binding interface [206]. To test this hypothesis, Waldron and Springer (2009) mutated alanine 28 to histidine (A28H), which fills up the space and opens the lobe in the lectin domain. Flow-based adhesion assays revealed that cells displaying the A28H mutated P-selectin relative to wild-type P-selectin, exhibited slower rolling on a PSGL-1 substrate at higher shear stresses, although no differences were noted in the low shear regime ($\tau_w \leq 0.2$ Pa) [206]. The dissociation constant (K_d) measured by surface plasmon resonance was 3- to 4-fold lower for mutated than wild-type P-selectin [206]. This increase in the binding affinity of A28H P-selectin for PSGL-1 provides evidence for an allosteric pathway through the lectin domain, which connects the conformational change at the lectin-EGF domains to the ligand-binding interface [186,206]. A simple allosteric model together with an equilibrium constant K_c describing the ratio of the two unbound conformations was introduced to explain the catch bond behavior of P-selectin-PSGL-1 binding [206]. Increasing the value of K_c favors the higher-affinity extended conformation, thereby resulting in enhancement of the overall binding affinity. In addition to the mechanistic interpretation provided by the ‘sliding-rebinding’ model [121,122], the ‘allosteric model’ suggests that force could act as an allosteric effector in the mechanochemistry of selectin-ligand bindings [186,206]. Similar force-induced conformational changes have been observed in integrins [9,73,175].

Simulation studies suggest that the catch-slip bond kinetics at the nanoscale level are primarily responsible for the shear-threshold phenomenon in which the extent of neutrophil rolling first increases and then decreases while monotonically increasing the wall shear stress [145]. Although shear-induced cell deformation can increase the contact area between the cell and the substrate, thereby enhancing the binding probability, numerical studies suggest that cell deformation plays a rather auxiliary role in the shear threshold phenomenon [145]. This notion is further supported by experimental observations showing that cell-free flow assays using purified selectins and their respective ligands can successfully recapitulate the shear threshold phenomenon [123,219]. In addition to the catch bond behavior, the effect of shear flow on the on-rate has been suggested to contribute to the shear threshold phenomenon [23,25]. Under the influence of a viscous flow and the presence of a vessel wall, the cell translational velocity is always larger than the surface tangential velocity, which results in a relative motion between the cell receptor and the immobilized ligand on the vessel wall [54]. This relative motion allows each cell receptor of a free-flowing cell to

potentially react with any counter-receptor present in its reactive zone, thereby increasing the receptor-ligand encounter rate for bond formation [23,25]. In addition to the relative sliding between cell receptors and immobilized ligands on the surface, Zhu and coworkers (2007) proposed two other transport mechanisms for the flow-enhanced bond formation between a free-flowing cell and the substrate: Brownian motion and molecular diffusion [220]. The Brownian motion causes a cell to move with a wavy trajectory perpendicular to the wall thereby altering the gap distance between receptors and immobilized ligands. Binding can only occur when a ligand locates within the reactive zone of a receptor on the free flowing cell [23]; as a result, the Brownian motion of the cell modulates the initial bond formation by inducing fluctuations in gap distance [220]. Although the movement of receptors and ligands is limited due to their anchorage on their respective cell/wall surfaces, receptors and ligands can still undergo rotational diffusion, which orients their binding sites for molecular docking [220]. The molecular diffusivity of selectins can be increased by enhancing the hinge flexibility of the lectin and EGF domains, such as by disrupting the Tyr37-Asn138 hydrogen bond in L-selectin [121]. Compared to wild-type L-selectin, microspheres bearing a more flexible L-selectin (N138G mutated) hinge display a higher tethering rate on PSGL-1-coated surfaces [121]. In addition, the greater hinge flexibility of mutated L-selectin further prolongs bond lifetimes at smaller forces, thereby lowering the shear threshold for rolling from 0.07 to 0.04 Pa [121]. Taken together, experimental and simulation studies collectively show that the origin of shear threshold phenomenon is caused primarily by the mechanical regulation of the association and dissociation rates.

4.1.3. Role of bond clusters in leukocyte rolling—It has been well documented that the spatial patterns of receptor-ligand bonds, in particular bond clusters, are significant factors in leukocyte rolling on P-selectin [56,81,87,152,173]. In neutrophils the bond clustering phenomenon is enabled by local concentrations of neutrophil microvilli visible as cell surface ridges [68,163], concentrations of PSGL-1 molecules (ligands) on microvilli tips [133], and local concentrations of P-selectin molecules (receptors) on the substrate. All three of these conditions are present prior to the beginning of a cell rolling process.

Two modeling studies suggest that the first two factors do not affect leukocyte rolling much. Shao and Xu [173] simulated an adhesion process (by cell-substrate contact, no rolling) for normal cells with ligands concentrated on the microvilli tips and smooth cells (no microvilli) with the same number of ligands distributed randomly on the cell's surface. In both cases the receptors were of the same density and randomly distributed on the substrate. They tested the receptor and ligand densities up to 3000 molecules/μm^2 and found that the ligand concentration on the microvilli tips did not affect the total number of adhesion events much. Pospieszalska et al. [152] conducted neutrophil rolling simulations by ETMA (Event-Tracking Model of Adhesion) for 941 microvilli per cell and 8 PSGL-1 dimers per microvillus (Case I) or 2,306 microvilli per cell and 4 PSGL-1 dimers per microvillus (Case II). In both cases, P-selectin at a site density of 150 molecules/μm^2 was distributed randomly on the substrate and the shear stress was 0.05 Pa. Each dimer could form one bond with P-selectin which was assumed to be monomeric [123]. Despite the drastic differences in microvillus and ligand distributions, the rolling for the two cases was similar when taking into consideration different number of PSGL-1 dimers per cell.

In a second simulation in the study by Shao and Xu [173], when the receptors at a fixed average density were randomly distributed on the substrate, or as random clusters of three molecules, or as random clusters of seven molecules, the number of adhesion events decreased with the increase in size of the cluster. Although *in vitro* rolling studies assume P-selectin to be randomly distributed on the substrate, recent studies have shown that P-selectin is preferentially presented as clusters of dimers in the clathrin-coated pits on EC and this clustering takes place through the interaction of the cytoplasmic domains of dimeric P-

selectin with clathrin-coated pits [129,168,170]. Even a random distribution does not imply that there are no P-selectin clusters. For example, assuming that P-selectin at 150 molecules/μm^2 is randomly distributed on a 100-μm^2 substrate, there is a 22.4% chance that an area of 0.02 μm^2 will contain a three-receptor cluster (Pospieszalska and Ley, unpublished data).

Figure 4a shows the positions of the bond receptor bases (places where the receptors are attached to the substrate) at a selected time point generated by ETMA. The plane xy represents the substrate, and the cell translates in the positive x-direction. The red colored circles indicate the receptor bases of load-bearing bonds. Despite a random distribution of receptors, there are three-load-bearing-bond clusters and one two-load-bearing-bond cluster (all four marked by ovals) with each cluster corresponding to a different microvillus. Figure 4b shows the history of the 11 bonds seen in Fig. 4a as load bearing. Each bond is represented by a horizontal segment with three points. The left point marks the time when the bond is formed, the middle point marks the time when the bond becomes load-bearing, and the right point marks the time when the bond dissociates. The bonds form and dissociate at different times, but all except one become load-bearing approximately at the same time. This causes a sudden increase in the total bond force acting on the cell, and the cell suddenly slows down or suddenly stops moving temporarily (the latter occurs in the case illustrated in Fig. 4, data not shown). That is a source, but not exclusively, of the jerky motion seen in cell rolling. Causing sudden reductions in the cell translational velocity and sudden cell stops is the most pronounced role of bond clusters.

4.1.4. Role of cell-substrate separation distance—The cell-substrate separation distance is defined as the minimum distance between the cell body and the substrate excluding the bendable microvilli (Fig. 5-insert). Unlike bond clusters (discussed in section 4.1.3), the cell-substrate separation is a consequence of cell rolling except during the initial state when the cell is freely floating in the medium. In ETMA simulations [152] conducted for neutrophils rolling on a P-selectin coated substrate (150 molecules/μm^2) at a wall shear stress of 0.05 Pa, a freely floating cell in shear flow approaches the substrate because of gravity to form a first PSGL-1-P-selectin bond. The simulations revealed that the cell-substrate distance varies following loading and dissociation of individual bonds during stable rolling. When at least one load-bearing bond was present, the cell was attached to the substrate resulting in a small separation distance with an average value of 0.16 μm [150,152]. This separation distance depends on the component of the total bond force perpendicular to the substrate and the net colloidal force [151], while the total bond force depends on the number of load-bearing bonds and the configuration of the loaded bonds and tethers in the footprint of a rolling neutrophil [150,152,165]. The dissociation of the last load-bearing bond leads to two possible outcomes: if no other bonds (not-loaded) are present, the cell-substrate separation distance will approach its initial value which is the separation distance for a freely flowing sphere near the wall, unless a new bond forms at the very beginning of the dissociation process. If there are other unloaded bonds present, then the increasing separation distance will result in loading of at least one of those bonds forcing the cell to return to the state of at least one load-bearing bond in the footprint. Thus, the gap between the cell and the substrate modulates cell rolling. During stable rolling, only the second possibility is realized. Usually many bonds form and dissociate without ever becoming load-bearing (31 - 44% reported in [152] which is in agreement with [165]). However, some of these bonds may become loaded when the cell-substrate separation suddenly increases, and prevents the cell from escaping from the vicinity of the substrate. An example of stable rolling generated using ETMA is given in Fig. 5 (Pospieszalska and Ley; unpublished data), which shows a scatter plot of the cell-substrate separation distance as a function of the cell translational velocity for Case II mentioned in section 4.1.3. A microvillus length of 0.2 μm and unstressed bond length of 0.07 μm were assumed [152]. Instantaneous changes in the separation distance are seen as individual traces. The trace

marked with an asterisk represents the first, gravity driven approach of the cell to the substrate. The almost vertical trace for the high translational velocities represents instantaneous changes in the separation distance when no load-bearing bonds were present and the cell attempted to depart from the substrate.

4.2. Cellular biomechanics

4.2.1. Whole cell deformation—Theoretical [36,37,72,84-86] and experimental [48,49,142,218] studies have shown that both molecular (i.e. kinetic and micromechanical properties of receptor-ligand pairs) and cellular properties such as cell deformation have a significant impact on the dynamics of rolling when cells are subjected to high yet physiologically relevant shear stresses. For instance, deformable polymorphonuclear leukocytes roll significantly slower and smoother than rigid microbeads coated with a similar density of selectin ligand molecules [142]. Bulk cell deformation is predicted to increase the contact area between the cell and substrate [33,49], as was recently confirmed experimentally [191]. The hydrodynamic loading of receptor-ligand bonds is also reduced due to a flattened cell shape [36,37,86].

A 3-D computational model of leukocyte rolling was proposed to simulate rolling of a PSGL-1-decorated deformable cell on a P-selectin-coated surface under flow [72]. In this model, the immersed boundary method (IBM) [146] was used to simulate motion of an elastic capsule near a plane wall in a linear shear field. The IBM was coupled to the Hookean spring model (Eq. 10-12) to simulate the force-dependent kinetics of receptor-ligand interactions [35], while the stochastic behavior of P-selectin-PSGL-1 bond formation and breakage was simulated by the Monte Carlo method [26,60]. The model successfully predicted that for a given shear rate, the extent of cell deformation and the cell-substrate contact area increase with decreasing cell membrane stiffness and thus increasing compliance. Furthermore, the rolling of more compliant cells is relatively smoother and slower compared to cells with stiffer membranes [72] which is in accord with experimental observations [142,218]. The average number of bonds for a cell as well as those for a single microvillus was found to increase with decreasing values of membrane stiffness which translates to increased deformability [72]. Along these lines, bond lifetimes decreased with increasing shear rate and also with increasing membrane stiffness [72]. More recently, this model was extended to incorporate the three different kinetic models of receptor-ligand binding (viz. Bell, Dembo and Evans two-pathway model) and to account for microvillus deformability [145]. These simulations predicted that the catch-slip bond behavior and to a lesser extent bulk cell deformation contribute to the shear-threshold phenomenon observed in the low shear regime. Moreover, cells bearing deformable rather than rigid microvilli rolled slower only at elevated P-selectin site densities and wall shear rates ($\geq 400\ sec^{-1}$). Another 3D computational model [84-85] of leukocyte rolling which assumes the cell to be a compound visoelastic drop (a viscoelastic nucleus covered with a thick layer of less viscoelastic cytoplasm) has shown that a cell with viscoelastic cytoplasm is more deformable than the one with Newtonian fluid-like cytoplasm when suitable parameters are used. Owing to the increased deformability, the hyrdrodynamic drag force and the torque acting on the rolling cell are significantly reduced for the viscoelastic cell resulting in more stable and smaller rolling velocity. The computational model in this study was based on the volume of fluid method coupled to the Hookean spring model [35] (Eqs. 10-12) for force-dependent receptor-ligand kinetics. Taken together, these computational studies suggest that the interplay of bulk cell deformation (mesoscale), microvillus deformability (microscale) and receptor-ligand binding kinetics (nanoscale) regulates cell rolling especially at elevated yet physiologically relevant shear stresses [145].

Quantitative dynamic footprinting (qDF) microscopy can be used to reconstruct the footprint of rolling neutrophils, which provides 3D locations of the microvilli tips as well as stretched lengths of the P-selectin-PSGL-1 bonds inside the cell-substrate contact area [191]. For a mouse neutrophil rolling on P-selectin at 0.6 Pa, the size of the footprint within 100 nm above the substrate was around 12 μm^2 which is about 4-fold larger than that previously estimated based on low-resolution *in vivo* measurements and modeling [33,152,191]. The large size of the footprint seems to be attributable to the cell deformation since a significantly smaller footprint (~3 μm^2) was obtained in ETMA simulations by assuming a spherical cell shape (comparison shown in Fig. 6) [150, 152]. In fact, the location of a stretched microvillus was reported as far as 3 μm behind the cell center in the qDF assay, which is longer than the value (<1 μm) estimated by ETMA simulation (Fig. 6) [152,191]. Contrary to ETMA applied to non-deformable cells, the compound viscoelastic model of leukocyte has been shown to have much larger footprints and the footprint size was shown to be inversely related to the cytoplasmic viscosity [84]. These observations support the concept that the membrane deformation as well as cytoplasmic viscoelasticity both play important roles in the dynamics of cell rolling under high shear stress [229]. This may explain the failure of the numerical models [22,88,150] which assume the cell to be a nondeformable sphere, to reproduce stable rolling at high shear stresses commonly observed *in vivo* [33,49].

4.2.2. Microvillus extension—Many living cells have an ability to form tubular surface protrusions in response to a low to moderate pulling force F(F < ~ 92 pN for neutrophils, Pospieszalska and Ley, unpublished data) applied locally to the cell membrane (Fig. 7b). If the force F is greater than the threshold force F_{th} (a non-zero pulling force below which the separation of the cell membrane from the cytoskeleton cannot occur), and acts for a sufficiently long time, a tether forms on the extension of the protrusion (Fig. 7c) [208]. The protrusion to tether transition is called the crossover, and is generally viewed in the literature as the termination of the protrusion's elongation [45,172,216]. The cellular protrusions and tethers (the latter are discussed in section 4.2.3) have been observed experimentally [16,45,65,71,142,154,155,166,167,172,191,215,216], analyzed theoretically [16,17,69,210], and modeled computationally [22,65,88,145,150,154,167,216,221]. In rolling neutrophils, pulling forces are applied to the tips of microvilli by molecular bonds formed between the microvilli and the substrate (Fig. 2). A protrusion formed at the tip of a microvillus is often described in literature as a microvillus extension (Fig. 7b).

Three models have been proposed for describing microvillus extension material and applied to pulling experiments involving PSGL-1-P-selectin bonds: an elastic model [172] represented by a spring shown in Fig. 8a, a Kelvin-Voigt viscoelastic model [150,216] represented by a spring and a dashpot connected in parallel shown in Fig. 8b, and a viscoelastic model composed of a Kelvin-Voigt unit connected in series with an elastic unit [154,216] shown in Fig. 8c. The parameters σ_{mv} and κ_{mv} are the spring constants for the corresponding springs, and η_{eff_mv} is the effective viscosity of the dashpot. The equation under each schematic representation gives the relation between the pulling force, F_{mv}, and the microvillus extension, L_{mv}. The extension L_{mv} under a constant pulling force F_{mv} is shown in Fig. 8d for F_{mv} = 45 pN, and the neutrophil parameters σ_{mv} = 43 pN μm^{-1} and η_{eff_mv} = 33 pN s μm^{-1} [150,172], and κ_{mv} = 800 pN μm^{-1} [154]. (The biophysical parameters and their symbols are defined in Table 2.)

As shown in Fig. 8d, the elastic model (Fig. 8a) does not represent the instantaneous changes in the microvillus extension under constant force F_{mv}, which have been observed experimentally. The Kelvin-Voigt viscoelastic model (Fig. 8b), describing the instantaneous changes in the microvillus extension, is consistent with the instantaneous experimental data of [172,216]. In the experiment of [172], the neutrophil is not completely immobilized, but

moves in a micropipette under a suction pressure. The third model (Fig. 8c) is proposed in [216] in the context of a pulling experiment where the neutrophil is held at the tip of the micropipette by a suction pressure. It has been shown [45] that a red blood cell held at the tip of a micropipette by suction pressure responds as a spring (an elastic response) to a pulling force with a spring constant defined by the suction pressure, micropipette radius, cell radius, and the radius of the outer spherical portion of the cell. Therefore, most likely, the additional spring in Fig. 8c, compared to Fig. 8b, does not represent the tether, but rather the elastic response of the neutrophil body reacting to the pulling force similar to the response of red blood cells.

The occurrence of a crossover, which is viewed as a termination of the microvillus extension and beginning of tether formation, seems to depend on the pulling pattern. Generally, it is assumed that the crossover occurs when there is a clear change in the shape of the pulling force as a function of time [45,172,216]. In the experiment of [172], the crossover occurs when the initially increasing tether pulling force becomes constant. In different pulling pattern experiments of [45,65,216], the crossover occurs when the apparently linear pulling force starts arching to approach a plateau force at long times. The apparently linear force is really not linear as it is expressed using an exponential function (Eq. A1 in [216]). The same applies to the extension of the microvillus, as seen in Eq. A2 in [216].

Based on the Kelvin-Voigt model, larger σ_{mv} and η_{eff_mv} (i.e. less extendable microvilli) result in faster cell rolling (Pospieszalska and Ley, unpublished data) because, overall, the less extendable microvillus results in a larger force ($F_{mv,1}$ in Fig. 2) on the bonds decreasing their life time. Thus the ability of microvilli to extend stabilizes the rolling adhesion in the presence of hydrodynamic shear forces by increasing the lifetime of selectin-ligand bonds. Three published cell rolling models consider the contribution of microvillus extension [22,145,152]. However, the role of tether extension in stabilizing neutrophil rolling has not been studied in detail.

4.2.3 Tether formation—As discussed in the previous section, when a bond pulling force F_{mv} is greater than the threshold force, F_{th}, and acts for a sufficiently long time, a tether starts to form on the tip of the microvillus. At that point the microvillus is elongated if F_{mv} is low to moderate. The biological nature of cellular tethers is not fully understood. The transition (a crossover) from microvillus elongation to tether formation is believed to occur when the cell membrane separates from the underlying cytoskeleton (Fig. 7c) and starts flowing around integral proteins embedded in the membrane and bound to the cytoskeleton nodes, and into the tether [16]. Long cellular membrane tethers were observed *in vivo* [182], studied in flow chambers and micropipette/laser trap experiments *in vitro* [16,39,45,65,71,140-142,154,155,166,167,172,191,215,216], and modeled *in silico* [22,88,145,150,216,221]. Recently, qDF microscopy has shown that a neutrophil rolling on P-selectin under high shear stress (0.6-0.8 Pa) forms 3-4 long tethers which can extend up to 16 μm behind the rolling cell (Fig. 9) [191]. The anchorage points of long tethers were visible in the qDF micrographs of rolling neutrophils (Fig. 9a) and the 3D reconstruction of the qDF footprints (Fig. 9b) revealed that the tether anchorage points are held to the substrate through stressed P-selectin-PSGL-1 bonds (L_{sep} = 125-175 nm).

Several studies led to the formulation of a theoretical framework for the tether phenomenon [16,17,69,210]. These studies resulted in a mathematical description of the tether dynamic equilibrium as a state of non-zero duration characterized by a constant tether pulling force, $F_{te} > 0$, and a constant tether extension rate, $\dot{L}_{te} = dL_{te}/dt > 0$, where L_{te} denotes the tether extension. Constant F_{te} and $\dot{L}_{te}$ of a dynamic equilibrium satisfy Eq. 16:

$$\dot{L}_{te} = \left[F_{te}{}^3 - F_{te}(F_{th})^2 \right] / \left[16\pi^3 (k_c)^2 d_{int} \ln (r_c F_{te}/2\pi k_c) \right] \quad (16)$$

In Eq. 16, $F_{te} > F_{th}$, r_c is the cell radius, k_c is the cell membrane curvature modulus, and d_{int} is the interfacial drag coefficient (i.e. the surface density of the bound integral proteins multiplied by the surface viscosity). Equation 16 is valid for 0.01 μm/s < $\dot{L}_{te}$ < $\dot{L}_c$, where $\dot{L}_c$ is the upper limit for the integral proteins to remain bound to the cytoskeleton ($\dot{L}_c \approx 100$ μm/s for neutrophils [17]). Equation 16 describes the relation between F_{te} and $\dot{L}_{te}$ exclusively for a tether in a dynamic equilibrium. However, there are pulling processes which demonstrate a crossover and no equilibrium.

So far, material properties of cellular tethers have been treated only phenomenologically. Three propositions for the tether material representation have been suggested in the literature based on agreement with at least one experiment. According to the first study [172], the force on the tether, F_{te}, can be defined as

$$F_{te}(t) = F_{th} + \eta_{eff\_te} \dot{L}_{te}(t) \quad (17)$$

where η_{eff_te} is the tether effective viscosity [22,150]. (Note that the factor preceding $\dot{L}_{te}(t)$ in Eq. 17 can be also found in literature in the form of $2\pi\eta_{eff}$ as in [69] where η_{eff} is referred as the effective viscosity). Equation 17 represents a viscous unit, $\eta_{eff\_te}\dot{L}_{te}(t)$, being pulled by a force of $F_{te}(t) - F_{th}$ (a force smaller than the pulling force), and shows that $\dot{L}_{te}$ is linearly dependent on F_{te} which is not true for tethers in dynamic equilibriums ($\dot{L}_{te}$ in Eq. 16 is a non-linearly increasing function of F_{te}). A second study [65] suggests that the force, F_{te}, on a neutrophil tether can be defined as:

$$F_{te}(t) = 60\left[\dot{L}_{1,te}(t) \quad \mu m^{-1} s \right]^{0.25} = \left[60\left(\mu m^{-1} \quad s\right)^{0.25} \dot{L}_{1,te}(t)^{-0.75} \right] \dot{L}_{1,te}(t) = kL_{2,te}(t) \quad (18)$$

F_{te} has the units of pN, $\dot{L}_{1,te}$ has the units of μm/s, and $L_{1,te} + L_{2,te} = L_{te}$. After singling out $\dot{L}_{1,te}(t$, the authors view their formula as a viscous-like unit of extension $L_{1,te}$ with its effective viscosity being a function of t, connected in series with an elastic unit of extension $L_{2,te}$ with spring constant k (not specified). The tether extension is the total extension of both units. When $\dot{L}_{te} = 0$, Eq. 18 yields $F_{te} = 0$ instead of $F_{te} = F_{th} \neq 0$. A correction to this discrepancy was suggested [30,171] that requires substituting $\dot{L}_{1,te}(t)$ in Eq. 18 with $\dot{L}_{te}(t) + a$ (no elastic unit), where $a > 0$ is a way that the corrected formula yields $F_{te} = F_{th}$ for $\dot{L}_{te} = 0$. The authors interpret $-a$ as the tether retraction velocity for $F_{te} = 0$. However, preliminary data obtained using qDF microscopy (Sundd, Pospieszalska and Ley; unpublished data) indicates that the retraction velocity may depend on the state of the tether in the pulling process when the pulling force F_{te} becomes zero. In Pospieszalska et al. [230] we propose to substitute the above three phenomenological formulations with a mathematically derived formula for the tether material.

Published modeling studies on neutrophil rolling on P-selectin that take microvillus deformation (i.e. microvillus extension and tether formation) into consideration use the elastic model in Fig. 8a [22,145] or the Kelvin-Voigt viscoelastic model in Fig. 8b [150] for microvillus extension, and Eq. 17 for tether formation [22,145,150]. All three studies [22,145,150] conclude that microvillus deformation reduces the cell translational velocity. The reduction is up to 35% for a shear rate of 400 s^{-1} and P-selectin site density of 150 molecules/μm^2, as reported in [145]. Lower translational velocities are the result of larger

number of bonds and longer bond lifetimes. The modeling work of [88] confirms that the microvillus deformation in rolling neutrophils results in increased P-selectin-PSGL-1 bond life times [88].

Tether elongation seems to depend on the pulling pattern. In the experiment of [172], a tether establishes a dynamic equilibrium already at crossover and stays in that equilibrium as long as the pulling process continues. In different pulling pattern experiments of [65,216] a tether approaches a dynamic equilibrium at long times. In an experiment with a constant tether loading rate the pulling force increases linearly and the tether cannot establish a dynamic equilibrium. A dynamic equilibrium creates favorable conditions for the survival of molecular bonds holding the tether in place, because the force on a bond is no longer increasing. The chance for a molecular bond to survive until a dynamic equilibrium of its tether is reached has not been established. However, the presence of very long tethers observed by qDF microscopy [191], and by other techniques [155,166], suggests that such bonds must exist.

5. Summary and concluding remarks

Neutrophil recruitment to sites of inflammation is mediated by selectin-dependent rolling. P- and E-selectin expressed on EC bind with intermediate affinity and high off-rates to their respective sialo-mucin ligands expressed on neutrophils. Forced bond dissociation in the presence of shear flow is balanced by rapid bond formation to mediate rolling interactions. PSGL-1, which is constitutively clustered on the tips of neutrophil microvilli, serves as the high-affinity ligand for all three selectins. The shearing fluid exerts a shear force and torque on the rolling neutrophil, which is balanced by the bond forces generated in the load-bearing bonds at the rear of the rolling neutrophil. Selectin-ligand molecular interactions have fast unstressed forward and reverse reaction rates. The reverse reaction rate is further modulated by the tensile bond force. At smaller bond forces, the reverse reaction rate may decrease with increasing force to reach a minimum value at an optimum force, and then increases with increasing force. During the first phase, the selectin-ligand bond is thought to behave as a ‘catch bond’ and during the second phase as a ‘slip bond’. The force-dependent receptor-ligand binding kinetics responsible for ‘slip’ bond behavior can be explained using the ‘Bell (1978)’ [15] or ‘Dembo (1988)’ [35] model. The ‘catch-slip’ transitional behavior is captured by Evans’ two-pathway model (2004) [46]. Based on crystal-structure data and molecular dynamics simulations, the ‘catch-slip’ bond behavior may be explained using the ‘sliding-rebinding mechanism’ [121,122] or the ‘allosteric model’ [186,206]. Both models assume an equilibrium between the ‘bent or closed’ and ‘open or extended’ confirmation of the lectin-EGF domain hinge in the selectin molecule. The equilibrium shifts towards the ‘open or extended’ form under applied tensile force, decreasing reverse reaction rate and increasing the lifetime of selectin-ligand bonds.

Neutrophil rolling is known to exhibit a shear threshold phenomenon, which is most pronounced in rolling mediated by L-selectin-PSGL-1 interactions. In *in vitro* flow chambers, neutrophils do not roll on PSGL-1 coated substrate below a threshold shear stress, and the rolling increases and becomes more stable as the shear stress is increased, reaches a maximum at an optimal shear stress, and then becomes faster and irregular with increasing shear stress. This behavior may be explained by a synergistic effect of the transport-enhanced tethering and ‘catch’ bond-enhanced rolling. Neutrophil rolling is also modulated by the presence of bond clusters in the footprint of a rolling cell. Numerical simulations show that the P-selectin-PSGL-1 bond clusters in the footprint of rolling neutrophils are responsible for the ‘jerky’ rolling motion. Hydrodynamic loading of a bond cluster causes the neutrophil to slow down suddenly or even stop temporarily. Numerical simulations have

also shown that the cell-substrate separation distance varies with the dissociation and loading of P-selectin-PSGL-1 bonds and correlates with the cell translational velocity.

Neutrophils rolling at high shear stress (> 0.6 Pa) flatten and create a larger footprint. This mesoscale deformation contributes to the ability of neutrophils to roll at relatively uniform velocities over a wide range of shear stresses by increasing the number of bonds in the footprint and decreasing the hydrodynamic force on the bonds. In addition to whole cell deformation, microvilli deformation (viscoelastic extension and formation of long membrane tethers) further facilitates neutrophil rolling at high shear stress by increasing the length of the moment arm, and thus decreasing the force acting on the bonds required to balance the hydrodynamic torque acting around the cell center. Reduced bond forces result in longer bond lifetimes, and thus more stable rolling at high shear stresses.

Although the biomechanics of leukocyte rolling have been studied extensively over the last two decades, the biomolecular and biophysical mechanisms that allow leukocytes to roll at venular shear stresses larger than 0.6 Pa both *in vivo* and *in vitro* are still elusive. Measurements of molecular and cellular parameters from *in vitro* and *in vivo* studies have facilitated the creation of several *in silico* models of leukocyte rolling. However, none of the currently available models predict leukocyte rolling at high venular shear stresses (0.6-3.5 Pa [33]) that are commonly observed *in vivo*. Quantitative dynamic footprinting used to visualize the footprint of neutrophils rolling in whole blood at high shear stress (τ_w > 0.6 Pa) revealed that the deformation of neutrophils results in a large footprint and formation of 3-4 long membrane tethers at the rear of the rolling neutrophil. These mechanisms may facilitate neutrophil rolling at high shear stresses.

Elucidation of the biophysical and structural mechanisms behind neutrophil rolling at high shear stress requires a theoretical model based on the measurements of qDF microsopy, which can describe whole cell deformation as well as long tether formation at venular shear stresses. Such a model does not exist currently, therefore, the relative contribution of long tethers and the stressed microvilli to neutrophil rolling at high shear stress cannot be estimated. The hydrodynamic shear force and torque acting on a rolling neutrophil are balanced by the forces acting on the long tethers and stressed microvilli. Although total force acting on all the stressed microvilli and the tethers combined can be easily estimated using the force balance with experimental measurement of structural parameters, the individual contribution of a single tether or a stressed microvilli has never been measured experimentally. A combination of qDF with traction force microscopy [158,178] may allow measurements of forces acting on individual microvilli or tethers. Theoretical models that capture both whole cell deformation and long tether formation, along with experimental studies that allow measurement of the microvillus or tether bond force are required for an improved understanding of the biomechanics behind leukocyte rolling at high shear stress.

Acknowledgments

This study was supported by American Heart Association postdoctoral fellowship 09POST2230093 (P.S.), NIH EB02185 (K.L.), and NIH/NCI R01 CA101135 (K.K.).

References

1. Addison W. Experimental and practical researches on the structure and function of blood corpuscles; on inflammation, and on the origin and nature of tubercules in the lungs. Trans. Provinc. Med. Surg. Ass. 1843; 11:223–306.
2. Afshar-Kharghan V, Diz-Kucukkaya R, Ludwig EH, et al. Human polymorphism of P-selectin glycoprotein ligand 1 attributable to variable numbers of tandem decameric repeats in the mucinlike region. Blood. 2001; 97:3306–3307. [PubMed: 11342464]

3. Alberts, B.; Bray, D.; Lewis, J., et al. Molecular biology of the cell. Garland Publishing, Inc.; New York: 1994.
4. Alon R, Chen S, Fuhlbrigge R, et al. The kinetics and shear threshold of transient and rolling interactions of L-selectin with its ligand on leukocytes. Proc. Natl. Acad. Sci. USA. 1998; 95:11631–11636. [PubMed: 9751717]
5. Alon R, Chen S, Puri KD, et al. The kinetics of L-selectin tethers and the mechanics of selectin-mediated rolling. J. Cell Biol. 1997; 138:1169–1180. [PubMed: 9281593]
6. Alon R, Fuhlbrigge RC, Finger EB, Springer TA. Interactions through L-selectin between leukocytes and adherent leukocytes nucleate rolling adhesions on selectins and VCAM-1 in shear flow. J. Cell. Biol. 1996; 135:849–865. [PubMed: 8909556]
7. Alon R, Hammer DA, Springer TA. Lifetime of the P-selectin-carbohydrate bond and its response to tensile force in hydrodynamic flow. Nature. 1995; 374:539–542. [PubMed: 7535385]
8. Arbones ML, Ord DC, Ley K, et al. Lymphocyte homing and leukocyte rolling and migration are impaired in L-selectin-deficient mice. Immunity. 1994; 1:247–260. [PubMed: 7534203]
9. Astrof NS, Salas A, Shimaoka M, et al. Importance of force linkage in mechanochemistry of adhesion receptors. Biochemistry. 2006; 45:15020–15028. [PubMed: 17154539]
10. Atherton A, Born GVR. Quantitative investigation of the adhesiveness of circulating polymorphonuclear leucocytes to blood vessel walls. J. Physiol. 1972; 222:447–474. [PubMed: 4624453]
11. Atherton A, Born GVR. Relationship between the velocity of rolling granulocytes and that of the blood flow in venules. J. Physiol. 1973; 233:157–165. [PubMed: 4759098]
12. Baisse B, Galisson F, Giraud S, et al. Evolutionary conservation of P-selectin glycoprotein ligand-1 primary structure and function. BMC Evol. Biol. 2007; 7:166. [PubMed: 17868453]
13. Bargatze RF, Kurk S, Butcher EC, Jutila MA. Neutrophils roll on adherent neutrophils bound to cytokine-induced endothelial cells via L-selectin on the rolling cells. J. Exp. Med. 1994; 180:1785–1792. [PubMed: 7525838]
14. Barkalow FJ, Barkalow KL, Mayadas TN. Dimerization of P-selectin in platelets and endothelial cells. Blood. 2000; 96:3070–3077. [PubMed: 11049986]
15. Bell GI. Models for the specific adhesion of cells to cells. Science. 1978; 200:618–627. [PubMed: 347575]
16. Borghi N, Brochard-Wyart F. Tether extrusion from red blood cells: integral proteins unbinding from cytoskeleton. J. Physiol. 2007; 93:1369–1379.
17. Brochard-Wyart F, Borghi N, Cuvelier D, Nassoy P. Hydrodynamic narrowing of tubes extruded from cells. Proc. Natl. Acad. Sci. USA. 2006; 103:7660–7663. [PubMed: 16679410]
18. Bullard DC, Kunkel EJ, Kubo H, et al. Infectious susceptibility and severe deficiency of leukocyte rolling and recruitment in E-selectin and P-selectin double mutant mice. J. Exp. Med. 1996; 183:2329–2336. [PubMed: 8642341]
19. Bullard DC, Qin L, Lorenzo I, et al. P-selectin/ICAM-1 double mutant mice: acute emigration of neutrophils into the peritoneum is completely absent but is normal into pulmonary alveoli. J. Clin. Invest. 1995; 95:1782–1788. [PubMed: 7535798]
20. Burns A, Bowden R, Abe Y, et al. P-selectin mediates neutrophil adhesion to endothelial cell borders. J. Leukoc. Biol. 1999; 65:299–306. [PubMed: 10080531]
21. Butcher EC. Leukocyte-endothelial cell recognition: three (or more) steps to specificity and diversity. Cell. 1991; 67:1033–1036. [PubMed: 1760836]
22. Caputo KE, Hammer DA. Effect of microvillus deformability on leukocyte adhesion explored using adhesive dynamics simulations. Biophys. J. 2005; 89:187–200. [PubMed: 15879471]
23. Caputo KE, Lee D, King MR, Hammer DA. Adhesive Dynamics Simulations of the Shear Threshold Effect for Leukocytes. Biophys. J. 2007; 92:787–797. [PubMed: 17085490]
24. Carlow DA, Gossens K, Naus S, et al. PSGL-1 function in immunity and steady state homeostasis. Immunol. Rev. 2009; 230:75–96. [PubMed: 19594630]
25. Chang KC, Hammer DA. The forward rate of binding of surface-tethered reactants: effect of relative motion between two surfaces. Biophys. J. 1999; 76:1280–1292. [PubMed: 10049312]

26. Chang KC, Tees DFJ, Hammer DA. The state diagram for cell adhesion under flow: leukocyte rolling and firm adhesion. Proc. Natl. Acad. Sci. USA. 2000; 97:11262–11267. [PubMed: 11005837]
27. Chen S, Springer TA. Selectin receptor-ligand bonds: formation limited by shear rate and dissociation governed by the Bell model. Proc. Natl. Acad. Sci. USA. 2001; 98:950–955. [PubMed: 11158576]
28. Chen S, Springer TA. An automatic braking system that stabilizes leukocyte rolling by an increase in selectin bond number with shear. J. Cell Biol. 1999; 144:185–200. [PubMed: 9885254]
29. Chen W, Evans EA, McEver RP, Zhu C. Monitoring receptor-ligand interactions between surfaces by thermal fluctuations. Biophys. J. 2008; 94:694–701. [PubMed: 17890399]
30. Chen Y, Yao DK, Shao JY. The Constitutive Equation for Membrane Tether Extraction. Ann. Biomed Eng. 2010; 38:3756–3765. [PubMed: 20614242]
31. Chesnutt BC, Smith DF, Raffler NA, et al. Induction of LFA-1-dependent neutrophil rolling on ICAM-1 by engagement of E-selectin. Microcirculation. 2006; 13:99–109. [PubMed: 16459323]
32. Chiang EY, Hidalgo A, Chang J, Frenette PS. Imaging receptor microdomains on leukocyte subsets in live mice. Nat. Methods. 2007; 4:219–222. [PubMed: 17322889]
33. Damiano ER, Westheider J, Tozeren A, Ley K. Variation in the velocity, deformation, and adhesion energy density of leukocytes rolling within venules. Circ. Res. 1996; 79:1122–1130. [PubMed: 8943950]
34. Dembo, M. On peeling an adherent cell from a surface. In: Goldstein, B.; Wofsy, C., editors. Some Mathematical Problems in Biology. Vol. 24. American Mathematical Society; Providence, RI: 1994. p. 51-77.
35. Dembo M, Torney DC, Saxman K, Hammer D. The reaction limited kinetics of membrane-to-surface adhesion and detachment. Proc. Roy. Soc London B Biological Sciences. 1988; 234:55–83.
36. Dong C, Cao J, Struble EJ, Lipowsky HH. Mechanics of leukocyte deformation and adhesion to endothelium in shear flow. Ann. Biomed. Eng. 1999; 27:298–312. [PubMed: 10374723]
37. Dong C, Lei XX. Biomechanics of cell rolling: shear flow, cell-surface adhesion, and cell deformability. J. Biomech. 2000; 33:35–43. [PubMed: 10609516]
38. Dutrochet, H. Recherches anatomiques et physiologiques sur la structure intime des animaux et des vegetaux, et sur leur motilite. J.-B. Baillière et Fils.; Paris: 1824.
39. Edmondson KE, Denney WS, Diamond SL. Neutrophil-bead collision assay: pharmacologically induced changes in membrane mechanics regulate the PSGL-1/P-selectin adhesion lifetime. Biophys. J. 2005; 89:3603–3614. [PubMed: 16100264]
40. Epperson TK, Patel KD, McEver RP, Cummings RD. Noncovalent association of P-selectin Glycoprotein ligand-1 and minimal determinants for binding to P-selectin. J. Biol. Chem. 2000; 275:7839–7853. [PubMed: 10713099]
41. Eppihimer MJ, Wolitzky B, Anderson DC, et al. Heterogeneity of expression of E- and P-selectins in vivo. Circ. Res. 1996; 79:560–569. [PubMed: 8781489]
42. Eriksson EE. No detectable endothelial- or leukocyte-derived L-selectin ligand activity on the endothelium in inflamed cremaster muscle venules. J. Leukoc. Biol. 2008; 84:93–103. [PubMed: 18381812]
43. Eriksson EE, Xie X, Werr J, et al. Importance of primary capture and L-selectin-dependent secondary capture in leukocyte accumulation in inflammation and atherosclerosis in vivo. J. Exp. Med. 2001; 194:205–217. [PubMed: 11457895]
44. Erlandsen SL, Hasslen SR, Nelson RD. Detection and spatial distribution of the beta 2 integrin (Mac-1) and L-selectin (LECAM-1) adherence receptors on human neutrophils by high-resolution field emission SEM. J. Histochem. Cytochem. 1993; 41:327–333. [PubMed: 7679125]
45. Evans E, Heinrich V, Leung A, Kinoshita K. Nano- to microscale dynamics of P-selectin detachment from leukocyte interfaces. I. Membrane separation from the cytoskeleton. Biophys. J. 2005; 88:2288–2298. [PubMed: 15653718]
46. Evans E, Leung A, Heinrich V, Zhu C. Mechanical switching and coupling between two dissociation pathways in a P-selectin adhesion bond. Proc. Natl. Acad. Sci. USA. 2004; 101:11281–11286. [PubMed: 15277675]

47. Evans EA, Calderwood DA. Forces and bond dynamics in cell adhesion. Science. 2007; 316:1148–1153. [PubMed: 17525329]
48. Finger E, Bruehl R, Bainton D, Springer T. A differential role for cell shape in neutrophil tethering and rolling on endothelial selectins under flow. J. Immunol. 1996; 157:5085–5096. [PubMed: 8943418]
49. Firrell JC, Lipowsky HH. Leukocyte margination and deformation in mesenteric venules of rat. Am. J. Physiol. Heart. Circ. Physiol. 1989; 256:H1667–H1674.
50. Frenette PS, Mayadas TN, Rayburn H, Hynes RO, Wagner DD. Susceptibility to infection and altered hematopoiesis in mice deficient in both P- and E-selectins. Cell. 1996; 84:563–574. [PubMed: 8598043]
51. Fritz J, Katopodis AG, Kolbinger F, Anselmetti D. Force-mediated kinetics of single P-selectin/ligand complexes observed by atomic force microscopy. Proc. Natl. Acad. Sci. USA. 1998; 95:12783–12288. [PubMed: 9788991]
52. Geng JG, Bevilacqua MP, Moore KL, McIntyre TM, Prescott SM, Kim JM, Bliss GA, Zimmerman GA, McEver RP. Rapid neutrophil adhesion to activated endothelium mediated by GMP-140. Nature. 1990; 343:757–760. [PubMed: 1689464]
53. Goetz DJ, El-Sabban ME, Pauli BU, Hammer DA. Dynamics of neutrophil rolling over stimulated endothelium in vitro. Biophys. J. 1994; 66:2202–2209. [PubMed: 7521229]
54. Goldman AJ, Cox RG, Brenner H. Slow viscous motion of a sphere parallel to a plane wall. II. Couette flow. Chem. Eng. Sci. 1967; 22:653–660.
55. Goldsmith HL, Spain S. Margination of leukocytes in blood flow through small tubes. Microvasc. Res. 1984; 27:204–222. [PubMed: 6708830]
56. Gopalakrishnan M, Forsten-Williams K, Nugent MA, Tauber UC. Effects of receptor clustering on ligand dissociation kinetics: theory and simulations. Biophys. J. 2005; 89:3686–3700. [PubMed: 16150967]
57. Gotsch U, Jager U, Dominis M, Vestweber D. Expression of P-selectin on endothelial cells is upregulated by LPS and TNF-alpha in vivo. Cell Adhes Commun. 1994; 2:7–14. [PubMed: 7526954]
58. Griffin JD, Spertini O, Ernst TJ, et al. Granulocyte-macrophage colony-stimulating factor and other cytokines regulate surface expression of the leukocyte adhesion molecule-1 on human neutrophils, monocytes, and their precursors. J. Immunol. 1990; 145:576–584. [PubMed: 1694883]
59. Hahne M, Jager U, Isenmann S, Hallmann R, Vestweber D. Five tumor necrosis factor-inducible cell adhesion mechanisms on the surface of mouse endothelioma cells mediate the binding of leukocytes. J. Cell Biol. 1993; 121:655–664. [PubMed: 7683689]
60. Hammer DA, Apte SM. Simulation of cell rolling and adhesion on surfaces in shear flow: general results and analysis of selectin-mediated neutrophil adhesion. Biophys. J. 1992; 63:35–57. [PubMed: 1384734]
61. Hanley W, McCarty O, Jadhav S, et al. Single molecule characterization of P-selectin/ligand binding. J. Biol. Chem. 2003; 278:10556–10561. [PubMed: 12522146]
62. Hanley WD, Wirtz D, Konstantopoulos K. Distinct kinetic and mechanical properties govern selectin-leukocyte interactions. J. Cell Sci. 2004; 117:2503–2511. [PubMed: 15159451]
63. Happel, J.; Brenner, H. Low Reynolds Number Hydrodynamics. Prentice-Hall, Inc.; Englewood Cliffs, N.J.: 1965. p. 553
64. Hattori R, Hamilton K, Fugate R, et al. Stimulated secretion of endothelial von Willebrand factor is accompanied by rapid redistribution to the cell surface of the intracellular granule membrane protein GMP-140. J. Biol. Chem. 1989; 264:7768–7771. [PubMed: 2470733]
65. Heinrich V, Leung A, Evans E. Nano- to microscale dynamics of P-selectin detachment from leukocyte interfaces. II. Tether flow terminated by P-selectin dissociation from PSGL-1. Biophys. J. 2005; 88:2299–2308. [PubMed: 15653735]
66. Hemmerich S, Bistrup A, Singer MS, et al. Sulfation of L-selectin ligands by an HEV-restricted sulfotransferase regulates lymphocyte homing to lymph nodes. Immunity. 2001; 15:237–247. [PubMed: 11520459]

67. Hidalgo A, Peired AJ, Wild MK, et al. Complete identification of E-selectin ligands on neutrophils reveals distinct functions of PSGL-1, ESL-1, and CD44. Immunity. 2007; 26:477–489. [PubMed: 17442598]
68. Hochmuth RM. Micropipette aspiration of living cells. J. Biomech. 2000; 33:15–22. [PubMed: 10609514]
69. Hochmuth RM, Shao JY, Dai J, Sheetz MP. Deformation and flow of membrane into tethers extracted from neuronal growth cones. Biophys. J. 1996; 70:358–369. [PubMed: 8770212]
70. Huang J, Chen J, Chesla SE, et al. Quantifying the effects of molecular orientation and length on two-dimensional receptor-ligand binding kinetics. J. Biol. Chem. 2004; 279:44915–44923. [PubMed: 15299021]
71. Hwang WC, Waugh RE. Energy of dissociation of lipid bilayer from the membrane skeleton of red blood cells. Biophys. J. 1997; 72:2669–2678. [PubMed: 9168042]
72. Jadhav S, Eggleton CD, Konstantopoulos K. A 3-D computational model predicts that cell deformation affects selectin-mediated leukocyte rolling. Biophys. J. 2005; 88:96–104. [PubMed: 15489302]
73. Jin M, Andricioaei I, Springer TA. Conversion between three conformational states of integrin I domains with a C-terminal pull spring studied with molecular dynamics. Structure. 2004; 12:2137–2147. [PubMed: 15576028]
74. Jung U, Bullard DC, Tedder TF, Ley K. Velocity differences between L- and P-selectin-dependent neutrophil rolling in venules of mouse cremaster muscle in vivo. Am. J. Physiol. Heart Circ. Physiol. 1996; 271:H2740–H2747.
75. Jung U, Ley K. Regulation of E-selectin, P-selectin, and intercellular adhesion molecule 1 expression in mouse cremaster muscle vasculature. Microcirculation. 1997; 4:311–319. [PubMed: 9219223]
76. Jung U, Ley K. Mice lacking two or all three selectins demonstrate overlapping and distinct funciton for each selectin. J. Immunol. 1999; 162:6755–6762. [PubMed: 10352295]
77. Jung U, Norman KE, Scharffetter-Kochanek K, Beaudet AL, Ley K. Transit time of leukocytes rolling through venules controls cytokine-induced inflammatory cell recruitment in vivo. J. Clin. Invest. 1998; 102:1526–1533. [PubMed: 9788965]
78. Jutila MA, Rott L, Berg EL, Butcher EC. Function and regulation of the neutrophil MEL-14 antigen in vivo: comparison with LFA-1 and MAC-1. J. Immunol. 1989; 143:3318–3324. [PubMed: 2553811]
79. Kadash KE, Lawrence MB, Diamond SL. Neutrophil string formation: Hydrodynamic thresholding and cellular deformation during cell collisions. Biophys. J. 2004; 86:4030–4039. [PubMed: 15189898]
80. Kansas GS. Selectins and their ligands: current concepts and controversies. Blood. 1996; 88:3259–3287. [PubMed: 8896391]
81. Karnik R, Hong S, Zhang H, et al. Nanomechanical control of cell rolling in two dimensions through surface patterning of receptors. Nano Lett. 2008; 8:1153–1158. [PubMed: 18321075]
82. Katayama Y, Hidalgo A, Chang J, et al. CD44 is a physiological E-selectin ligand on neutrophils. J. Exp. Med. 2005; 201:1183–1189. [PubMed: 15824084]
83. Kawashima H, Petryniak B, Hiraoka N, et al. N-acetylglucosamine-6-O-sulfotransferases 1 and 2 cooperatively control lymphocyte homing through L-selectin ligand biosynthesis in high endothelial venules. Nat. Immunol. 2005; 6:1096–1104. [PubMed: 16227985]
84. Khismatullin, DB. The cytoskeleton and deformability of white blood cells. Leukocyte Adhesion. Ley, K., editor. Vol. 64. Academic Press; San Diego: 2009. p. 47-111.
85. Khismatullin DB, Truskey GA. Three-dimensional numerical simulation of receptor-mediated leukocyte adhesion to surfaces: Effects of cell deformability and viscoelasticity. Phys. Fluids. 2005; 17:031505, 1–21.
86. Khismatullin DB, Truskey GA. A 3D numerical study of the effect of channel height on leukocyte deformation and adhesion in parallel-plate flow chambers. Microvasc. Res. 2004; 68:188–202. [PubMed: 15501238]

87. Kim MB, Sarelius IH. Role of shear forces and adhesion molecule distribution on P-selectin-mediated leukocyte rolling in postcapillary venules. Am. J. Physiol. Heart Circ. Physiol. 2004; 287:H2705–2711. [PubMed: 15331369]

88. King MR, Heinrich V, Evans E, Hammer DA. Nano-to-micro scale dynamics of P-selectin detachment from leukocyte interfaces. III. Numerical simulation of tethering under flow. Biophys. J. 2005; 88:1676–1683. [PubMed: 15574709]

89. Kishimoto TK, Jutila MA, Berg EL, Butcher EC. Neutrophil Mac-1 and MEL-14 adhesion proteins inversely regulated by chemotactic factors. Science. 1989; 245:1238–1241. [PubMed: 2551036]

90. Klopocki AG, Yago T, Mehta P, et al. Replacing a lectin domain residue in L-selectin enhances binding to P-selectin glycoprotein ligand-1 but not to 6-sulfo-sialyl Lewis x. J. Biol. Chem. 2008; 283:11493–11500. [PubMed: 18250165]

91. Konstantopoulos K, Hanley WD, Wirtz D. Receptor–ligand binding: 'catch' bonds finally caught. Curr. Biol. 2003; 13:R611–R613. [PubMed: 12906816]

92. Konstantopoulos K, Kukreti S, McIntire LV. Biomechanics of cell interactions in shear fields. Adv. Drug Deliv. Rev. 1998; 33:141–164. [PubMed: 10837657]

93. Krasik EF, Hammer DA. A Semianalytic Model of Leukocyte Rolling. Biophys. J. 2004; 87:2919–2930. [PubMed: 15315955]

94. Kunkel EJ, Chomas JE, Ley K. Role of primary and secondary capture for leukocyte accumulation in vivo. Circ. Res. 1998; 82:30–38. [PubMed: 9440702]

95. Kunkel EJ, Dunne JL, Ley K. Leukocyte arrest during cytokine-dependent inflammation in vivo. J. Immunol. 2000; 164:3301–3308. [PubMed: 10706723]

96. Kunkel EJ, Jung U, Bullard DC, et al. Absence of trauma-induced leukocyte rolling in mice deficient in both P-selectin and intercellular adhesion molecule 1. J. Exp. Med. 1996; 183:57–65. [PubMed: 8551244]

97. Kunkel EJ, Ley K. Distinct Phenotype of E-Selectin–Deficient Mice: E-Selectin Is Required for Slow Leukocyte Rolling In Vivo. Circ. Res. 1996; 79:1196–1204. [PubMed: 8943958]

98. Kuwano Y, Spelten O, Zhang H, et al. Rolling on E- or P-selectin induces the extended but not high-affinity conformation of LFA-1 in neutrophils. Blood. 2010; 116:617–624. [PubMed: 20445017]

99. Labow MA, Norton CR, Rumberger JM, et al. Characterization of E-selectin-deficient mice: demonstration of overlapping function of the endothelial selectins. Immunity. 1994; 1:709–720. [PubMed: 7541306]

100. Langer HF, Chavakis T. Leukocyte-endothelial interactions in inflammation. J. Cell. Mol. Med. 2009; 13:1211–1220. [PubMed: 19538472]

101. Lawrence MB, Bainton DF, Springer TA. Neutrophil tethering to and rolling on E-selectin are separable by requirement for L-selectin. Immunity. 1994; 1:137–145. [PubMed: 7534197]

102. Lawrence MB, Kansas GS, Kunkel EJ, Ley K. Threshold levels of fluid shear promote leukocyte adhesion through selectins (CD62L,P,E). J. Cell Biol. 1997; 136:717–727. [PubMed: 9024700]

103. Lawrence MB, Smith CW, Eskin SG, McIntire LV. Effect of venous shear stress on CD18-mediated neutrophil adhesion to cultured endothelium. Blood. 1990; 75:227–237. [PubMed: 1967215]

104. Lawrence MB, Springer TA. Neutrophils roll on E-selectin. J. Immunol. 1993; 151:6338–6346. [PubMed: 7504018]

105. Lawrence MB, Springer TA. Leukocytes roll on a selectin at physiological flow rates: distinction from and prerequisite for adhesion through integrins. Cell. 1991; 65:859–874. [PubMed: 1710173]

106. Lenter M, Levinovitz A, Isenmann S, Vestweber D. Monospecific and common glycoprotein ligands for E- and P-selectin on myeloid cells. J. Cell Biol. 1994; 125:471–481. [PubMed: 7512971]

107. Lepännen A, Mehta P, Ouyang Y-B, Ju T, Helin J, Moore KL, Die I.v. Canfield WM, McEver RP, Cummings RD. A novel glycosulfopeptide binds to P-selectin and inhibits leukocyte adhesion to P-selectin. J. Biol. Chem. 1999; 274:24838–24848. [PubMed: 10455156]

108. Leppänen A, White SP, Helin J, McEver RP, Cummings RD. Binding of glycosulfopeptides to P-selectin requires stereospecific contributions of individual tyrosine sulfate and sugar residues. Journal of Biological Chemistry. 2000; 275:39569–39578. [PubMed: 10978329]
109. Leppanen A, Yago T, Otto VI, et al. Model glycosulfopeptides from P-selectin glycoprotein ligand-1 require tyrosine sulfation and a core 2-branched O-glycan to bind to L-selectin. J. Biol. Chem. 2003; 278:26391–26400. [PubMed: 12736247]
110. Levin JD, Ting-Beall HP, Hochmuth RM. Correlating the kinetics of cytokine-induced E-selectin adhesion and expression on endothelial cells. Biophys. J. 2001; 80:656–667. [PubMed: 11159434]
111. Ley K, Bullard DC, Arbones ML, Bosse R, Vestweber D, Tedder TF, Beaudet AL. Sequential contribution of L- and P-selectin to leukocyte rolling in vivo. J Exp Med. 1995; 181:669–675. [PubMed: 7530761]
112. Ley K, Laudanna C, Cybulsky MI, Nourshargh S. Getting to the site of inflammation: the leukocyte adhesion cascade updated. Nat Rev Immunol. 2007; 7:678–689. [PubMed: 17717539]
113. Ley K, Tedder TF, Kansas GS. L-selectin can mediate leukocyte rolling in untreated mesenteric venules in vivo independent of E- or P-selectin. Blood. 1993; 82:1632–1638. [PubMed: 7689875]
114. Ley K, Zakrzewicz A, Hanski C, Stoolman LM, Kansas GS. Sialylated O-glycans and L-selectin sequentially mediate myeloid cell rolling in vivo. Blood. 1995; 85:3727–3735. [PubMed: 7540070]
115. Li F, Erickson HP, James JA, Moore KL, Cummings RD, McEver RP. Visualization of P-selectin glycoprotein ligand-1 as a highly extended molecule and mapping of protein epitopes for monoclonal antibodies. J. Biol. Chem. 1996; 271:6342–6348. [PubMed: 8626430]
116. Li F, Wilkins PP, Crawley S, Weinstein J, Cummings RD, McEver RP. Post-translational modifications of recombinant P-selectin glycoprotein ligand-1 required for binding to P- and E-selectin. J. Biol. Chem. 1996; 271:3255–3264. [PubMed: 8621728]
117. Lim Y-C, Snapp K, Kansas GS, Camphausen R, Ding H, Luscinskas FW. Important contributions of P-selectin glycoprotein ligand-1-mediated secondary capture to human monocyte adhesion to P-selectin, E-selectin, and TNF-α-activated endothelium under flow in vitro. J. Immunol. 1998; 161:2501–2508. [PubMed: 9725249]
118. Lindbom L, Xie X, Raud J, Hedqvist P. Chemoattractant-induced firm adhesion of leukocytes to vascular endothelium in vivo is critically dependent on initial leukocyte rolling. Acta Physiol. Scand. 1992; 146:415–421. [PubMed: 1492559]
119. Linden MD, Jackson DE. Platelets: pleiotropic roles in atherogenesis and atherothrombosis. Int. J. Biochem. Cell Biol. 2010; 42:1762–1766. [PubMed: 20673808]
120. Liu, W.-j.; Ramachandran, V.; Kang, J., et al. Identification of N-terminal residues on P-selectin glycoprotein ligand-1 required for binding to P-selectin. J. Biol. Chem. 1998; 273:7078–7087. [PubMed: 9507018]
121. Lou J, Yago T, Klopocki AG, Mehta P, et al. Flow-enhanced adhesion regulated by a selectin interdomain hinge. J. Biol. Chem. 2006; 174:1107–1117.
122. Lou J, Zhu C. A structure-based sliding-rebinding mechanism for catch bonds. Biophys. J. 2007; 92:1471–1485. [PubMed: 17142266]
123. Marshall BT, Long M, Piper JW, et al. Direct observation of catch bonds involving cell-adhesion molecules. Nature. 2003; 423:190–193. [PubMed: 12736689]
124. Martinez M, Joffraud M, Giraud S, et al. Regulation of PSGL-1 interactions with L-selectin, P-selectin, and E-selectin: role of human fucosyltransferase-IV and -VII. J. Biol. Chem. 2005; 280:5378–5390. [PubMed: 15579466]
125. Mayadas TN, Johnson RC, Rayburn H, Hynes RO, Wagner DD. Leukocyte rolling and extravasation are severely compromised in P selectin-deficient mice. Cell. 1993; 74:541–554. [PubMed: 7688665]
126. McEver RP. Rolling back neutrophil adhesion. Nat. Immunol. 2010; 11:282–284. [PubMed: 20300135]
127. McEver RP. Selectins: lectins that initiate cell adhesion under flow. Curr. Opin. Cell Biol. 2002; 14:581–586. [PubMed: 12231353]

128. McEver RP, Moore KL, Cummings RD. Leukocyte trafficking mediated by selectin-carbohydrate interactions. J. Biol. Chem. 1995; 270:11025–11028. [PubMed: 7538108]
129. McEver RP, Zhu C. Rolling cell adhesion. Annu. Rev. Cell. Dev. Biol. 2010; 26:363–396. [PubMed: 19575676]
130. Mehta P, Cummings RD, McEver RP. Affinity and kinetic analysis of P-selectin binding to P-selectin glycoprotein ligand-1. J. Biol. Chem. 1998; 273:32506–32513. [PubMed: 9829984]
131. Mitoma J, Bao X, Petryanik B, et al. Critical functions of N-glycans in L-selectin-mediated lymphocyte homing and recruitment. Nat. Immunol. 2007; 8:409–418. [PubMed: 17334369]
132. Moore KL, Eaton SF, Lyons DE, et al. The P-selectin glycoprotein ligand form human neutrophils displays sialylated, fucosylated, O-linked poly-N-acetyllactosamine. J. Biol. Chem. 1994; 269:23318–23327. [PubMed: 7521878]
133. Moore KL, Patel KD, Bruehl RE, et al. P-selectin glycoprotein ligand-1 mediates rolling of human neutrophils on P-selectin. J. Biol. Chem. 1995; 128:661–671.
134. Muller WA. Leukocyte-endothelial cell interactions in the inflammatory response. Lab. Invest. 2002; 82:521–533. [PubMed: 12003992]
135. Nicholson MW, Barclay AN, Singer MS, et al. Affinity and kinetic analysis of L-selectin (CD62L) binding to glycosylation-dependent cell-adhesion molecule-1. J. Biol. Chem. 1998; 273:763–770. [PubMed: 9422729]
136. Nimrichter L, Burdick MM, Aoki K, et al. E-selectin receptors on human leukocytes. Blood. 2008; 112:3744–3752. [PubMed: 18579791]
137. Nobis U, Pries AR, Cokelet GR, Gaehtgens P. Radial distribution of white cells during blood flow in small tubes. Microvasc. Res. 1985; 29:295–304. [PubMed: 3999988]
138. Norman KE, Katopodis AG, Thoma G, et al. P-selectin glycoprotein ligand-1 supports rolling on E- and P-selectin in vivo. Blood. 2000; 96:3585–3591. [PubMed: 11071658]
139. Norman KE, Moore KL, McEver RP, Ley K. Leukocyte rolling in vivo is mediated by P-selectin glycoprotein ligand-1. Blood. 1995; 86:4417–4421. [PubMed: 8541529]
140. Oh H, Diamond SL. Ethanol enhances neutrophil membrane tether growth and slows rolling on P-selectin but reduces capture from flow and firm arrest on IL-1-treated endothelium. J. Immunol. 2008; 181:2472–2482. [PubMed: 18684938]
141. Oh H, Mohler ER III, Tian A, et al. Membrane cholesterol is a biomechanical regulator of neutrophil adhesion. Arterioscler. Thromb. Vasc. Biol. 2009; 29:1290–1297. [PubMed: 19667108]
142. Park EYH, Smith MJ, Stropp ES, et al. Comparison of PSGL-1 microbead and neutrophil rolling: microvillus elongation stabilizes P-selectin bond clusters. Biophys. J. 2002; 82:1835–1847. [PubMed: 11916843]
143. Paschall CD, Lawrence MB. L-selectin shear thresholding modulates leukocyte secondary capture. Ann. Biomed. Eng. 2008; 36:622–631. [PubMed: 18299990]
144. Patel KD, Nollert MU, McEver RP. P-selectin must extend a sufficient length from the plasma membrane to mediate rolling of neutrophils. J. Cell Biol. 1995; 131:1893–1902. [PubMed: 8557755]
145. Pawar P, Jadhav S, Eggleton CD, Konstantopoulos K. Roles of cell and microvillus deformation and receptor-ligand binding kinetics in cell rolling. Am. J. Physiol. Heart Circ. Physiol. 2008; 295:H1439–H1450. [PubMed: 18660437]
146. Peskin CS, McQueen DM. A 3-dimensional computational method for blood-flow in the heart. 1. Immersed elastic fibers in a viscous incompressible f.luid. J. Comput. Phys. 1989; 81:372–405.
147. Petri B, Phillipson M, Kubes P. The physiology of leukocyte recruitment: an in vivo perspective. J Immunol. 2008; 180:6439–6446. [PubMed: 18453558]
148. Phan UT, Waldron TT, Springer TA. Remodeling of the lectin-EGF-like domain interface in P- and L-selectin increases adhesiveness and shear resistance under hydrodynamic force. Nat. Immunol. 2006; 7:883–889. [PubMed: 16845394]
149. Phillipson M, Heit B, Colarusso P, et al. Intraluminal crawling of neutrophils to emigration sites: a molecularly distinct process from adhesion in the recruitment cascade. J. Exp. Med. 2006; 203:2569–2575. [PubMed: 17116736]

150. Pospieszalska MK, Ley K. Dynamics of microvillus extension and tether formation in rolling leukocytes. Cell. Mol. Bioeng. 2009; 2:207–217. [PubMed: 20046963]
151. Pospieszalska, MK.; Ley, K. Modeling leukocyte rolling, chapter 8. In: Ley, K., editor. Leukocyte adhesion. Vol. 64. Elsevier; San Diego: 2009. p. 221-273.
152. Pospieszalska MK, Zarbock A, Pickard JE, Ley K. Event-tracking model of adhesion identifies load-bearing bonds in rolling leukocytes. Microcirculation. 2009; 16:115–130. [PubMed: 19023690]
153. Pouyani T, Seed B. PSGL-1 recognition of P-selectin is controlled by a tyrosine sulfation consensus at the PSGL-1 amino terminus. Cell. 1995; 83:333–343. [PubMed: 7585950]
154. Python JL, Wilson KO, Snook JH, et al. The viscoelastic properties of microvilli are dependent upon the cell-surface molecule. Biochem. Biophys. Res. Commun. 2010; 397:621–625. [PubMed: 20570653]
155. Ramachandran V, Williams M, Yago T, et al. Dynamic alterations of membrane tethers stabilize leukocyte rolling on P-selectin. Proc. Natl. Acad. Sci. USA. 2004; 101:13519–13524. [PubMed: 15353601]
156. Ramachandran V, Yago T, Epperson TK, et al. Dimerization of a selectin and its ligand stabilizes cell rolling and enhances tether strength in shear flow. Proc. Natl. Acad. Sci. USA. 2001; 98:10166–10171. [PubMed: 11481445]
157. Rosen SD. Ligands for L-selectin: homing, inflammation, and beyond. Annu. Rev. Immunol. 2004; 22:129–156. [PubMed: 15032576]
158. Sabass B, Gardel ML, Waterman CM, Schwarz US. High resolution traction force microscopy based on experimental and computational advances. Biophys. J. 2008; 94:207–220. [PubMed: 17827246]
159. Sako D, Chang XJ, Barone KM, et al. Expression cloning of a functional glycoprotein ligand for P-selectin. Cell. 1993; 75:1179–1186. [PubMed: 7505206]
160. Sanders WE, Wilson RW, Ballantyne CM, Beaudet AL. Molecular cloning and analysis of *in vivo* expression of murine P-selectin. Blood. 1992; 80:795–800. [PubMed: 1379089]
161. Sarangapani KK, Yago T, Klopocki AG, et al. Low force decelerates L-selectin dissociation from P-selectin glycoprotein ligand-1 and endoglycan. J. Biol. Chem. 2004; 279:2291–2298. [PubMed: 14573602]
162. Schaff UY, Xing MM, Lin KK, et al. Vascular mimetics based on microfluidics for imaging the leukocyte--endothelial inflammatory response. Lab Chip. 2007; 7:448–456. [PubMed: 17389960]
163. Schmid-Schönbein G, Shih Y, Chien S. Morphometry of human leukocytes. Blood. 1980; 56:866–875. [PubMed: 6775712]
164. Schmid-Schonbein GW, Usami S, Skalak R, Chien S. The interaction of leukocytes and erythrocytes in capillary and postcapillary vessels. Microvasc. Res. 1980; 19:45–70. [PubMed: 7360047]
165. Schmidt BJ, Papin JA, Lawrence MB. Nano-motion dynamics are determined by surface-tethered selectin mechanokinetics and bond formation. PLoS Comput. Biol. 2009; 5:e1000612. [PubMed: 20019797]
166. Schmidtke DW, Diamond SL. Direct observation of membrane tethers formed during neutrophil attachment to platelets or P-selectin under physiological flow. J. Cell Biol. 2000; 149:719–729. [PubMed: 10791984]
167. Schmitz J, Benoit M, Gottschalk KE. The viscoelasticity of membrane tethers and its importance for cell adhesion. Biophys. J. 2008; 95:1448–1459. [PubMed: 18456832]
168. Setiadi H, McEver RP. Signal-dependent distribution of cell surface P-selectin in clathrin-coated pits affects leukocyte rolling under flow. J. Cell Biol. 2003; 163:1385–1395. [PubMed: 14676308]
169. Setiadi H, McEver RP. Clustering endothelial E-selectin in clathrin-coated pits and lipid rafts enhances leukocyte adhesion under flow. Blood. 2008; 111:1989–1998. [PubMed: 18029551]
170. Setiadi H, Sedgewick G, Erlandsen SL, McEver RP. Interaction of the cytoplasmic domain of P-selectin with clathrin-coated pits enhance leukocyte adhesion under flow. J. Cell Biol. 1998; 142:859–871. [PubMed: 9700172]

171. Shao, J-Y. Biomechanics of leukocyte and endothelial cell surface, chapter 2. In: Ley, K., editor. Leukocyte adhesion. Vol. 64. Elsevier; San Diego: 2009. p. 25-45.
172. Shao J-Y, Ting-Beall HP, Hochmuth RM. Static and dynamic lengths of neutrophil microvilli. Proc. Natl. Acad. Sci. USA. 1998; 95:6797–6802. [PubMed: 9618492]
173. Shao JY, Xu G. The adhesion between a microvillus-bearing cell and a ligand-coated substrate: a Monte Carlo study. Ann. Biomed. Eng. 2007; 35:397–407. [PubMed: 17151923]
174. Shigeta A, Matsumoto M, Tedder TF, et al. An L-selectin ligand distinct from P-selectin glycoprotein ligand-1 is expressed on endothelial cells and promotes neutrophil rolling in inflammation. Blood. 2008; 112:4915–4923. [PubMed: 18818390]
175. Shimaoka M, Xiao T, Liu JH, et al. Structures of the alpha L I domain and its complex with ICAM-1 reveal a shape-shifting pathway for integrin regulation. Cell. 2003; 112:99–111. [PubMed: 12526797]
176. Simon SI, Green CE. Molecular mechanics and dynamics of leukocyte recruitment during inflammation. Annu. Rev. Biomed. Eng. 2005; 7:151–185. [PubMed: 16004569]
177. Smith CW, Kishimoto TK, Abbassi O, et al. Chemotactic factors regulate lectin adhesion molecule 1 (LECAM-1)-dependent neutrophil adhesion to cytokine-stimulated endothelial cells in vitro. J. Clin. Invest. 1991; 87:609–618. [PubMed: 1991844]
178. Smith LA, Aranda-Espinoza H, Haun JB, et al. Neutrophil traction stresses are concentrated in the uropod during migration. Biophys. J. 2007; 92:L58–L60. [PubMed: 17218464]
179. Smith MJ, Berg EL, Lawrence MB. A direct comparison of selectin-mediated transient, adhesive events using high temporal resolution. Biophys. J. 1999; 77:3371–3383. [PubMed: 10585960]
180. Smith ML, Sperandio M, Galkina EV, Ley K. Autoperfused mouse flow chamber reveals synergistic neutrophil accumulation through P-selectin and E-selectin. J. Leukoc. Biol. 2004; 76:985–993. [PubMed: 15075351]
181. Somers WS, Tang J, Shaw GD, Camphausen RT. Insights into the molecular basis of leukocyte tethering and rolling revealed by structures of P- and E-selectin bound to sLe^X and PSGL-1. Cell. 2000; 103:467–479. [PubMed: 11081633]
182. Sperandio M, Smith ML, Forlow SB, et al. P-selectin glycoprotein ligand-1 mediates L-selectin-dependent leukocyte rolling in venules. J. Exp. Med. 2003; 197:1355–1363. [PubMed: 12756271]
183. Sperandio M, Thatte A, Foy D, et al. Severe impairment of leukocyte rolling in venules of core 2 glucosaminyltransferase-deficient mice. Blood. 2001; 97:3812–3819. [PubMed: 11389021]
184. Spertini O, Cordey AS, Monai N, et al. P-selectin glycoprotein ligand 1 is a ligand for L-selectin on neutrophils, monocytes, and CD34+ hematopoietic progenitor cells. J. Cell Biol. 1996; 135:523–531. [PubMed: 8896607]
185. Springer TA. Adhesion receptors of the immune system. Nature. 1990; 346:425–434. [PubMed: 1974032]
186. Springer TA. Structural basis for selectin mechanochemistry. Proc. Natl. Acad. Sci. USA. 2009; 106:91–96. [PubMed: 19118197]
187. Springer TA. Traffic signals for lymphocyte recirculation and leukocyte emigration: the multistep paradigm. Cell. 1994; 76:301–314. [PubMed: 7507411]
188. St Hill CA, Alexander SR, Walcheck B. Indirect capture augments leukocyte accumulation on P-selectin in flowing whole blood. J. Leukoc. Biol. 2003; 73:464–471. [PubMed: 12660221]
189. Steegmaier M, Borges E, Berger J, et al. The E-selectin-ligand ESL-1 is located in the Golgi as well as on microvilli on the cell surface. J. Cell Sci. 1997; 110:687–694. [PubMed: 9099943]
190. Subramaniam M, Saffaripour S, Watson SR, et al. Reduced recruitment of inflammatory cells in a contact hypersensitivity response in P-selectin-deficient mice. J. Exp. Med. 1995; 181:2277–2282. [PubMed: 7539046]
191. Sundd P, Gutierrez E, Pospieszalska MK, et al. Quantitative dynamic footprinting microscopy reveals mechanisms of neutrophil rolling. Nat. Methods. 2010; 7:821–824. [PubMed: 20871617]
192. Tauxe C, Xie X, Joffraud M, et al. P-selectin glycoprotein ligand-1 decameric repeats regulate selectin-dependent rolling under flow conditions. J. Biol. Chem. 2008; 283:28536–28545. [PubMed: 18713749]

193. Tedder TF, Steeber DA, Chen A, Engel P. The selectins: vascular adhesion molecules. FASEB J. 1995; 9:866–873. [PubMed: 7542213]

194. Tedder TF, Steeber DA, Pizcueta P. L-selectin-deficient mice have impaired leukocyte recruitment into inflammatory sites. J Exp. Med. 1995; 181:2259–2264. [PubMed: 7539045]

195. Tees DFJ, Waugh RE, Hammer DA. A microcantilever device to assess the effect of force on the lifetime of selectin-carbohydrate bonds. Biophys. J. 2001; 80:668–682. [PubMed: 11159435]

196. Tözeren A, Ley K. How do selectins mediate leukocyte rolling in venules? Biophys. J. 1992; 63:700–709. [PubMed: 1420908]

197. Tu L, Murphy PG, Li X, Tedder TF. L-selectin ligands expressed by human leukocytes are HECA-452 antibody-defined carbohydrate epitopes preferentially displayed by P-selectin glycoprotein ligand-1. J. Immunol. 1999; 163:5070–5078. [PubMed: 10528213]

198. Uchimura K, Gauguet JM, Singer MS, et al. A major class of L-selectin ligands is eliminated in mice deficient in two sulfotransferases expressed in high endothelial venules. Nat. Immunol. 2005; 6:1105–1113. [PubMed: 16227986]

199. Ushiyama S, Laue T, Moore K, et al. Structural and functional characterization of monomeric soluble P- selectin and comparison with membrane P-selectin. J. Biol. Chem. 1993; 268:15229–15237. [PubMed: 7686912]

200. Vestweber D, Blanks JE. Mechanisms that regulate the function of the selectins and their ligands. Physiol. Rev. 1999; 79:181–213. [PubMed: 9922371]

201. von Andrian UH, Chambers JD, McEvoy LM, et al. Two-step model of leukocyte-endothelial cell interaction in inflammation: distinct roles for LECAM-1 and the leukocyte beta 2 integrins in vivo. Proc. Natl. Acad. Sci. USA. 1991; 88:7538–7542. [PubMed: 1715568]

202. von Andrian UH, Hasslen SR, Nelson RD, Erlandsen SL, Butcher EC. A central role for microvillous receptor presentation in leukocyte adhesion under flow. Cell. 1995; 82:989–999. [PubMed: 7553859]

203. Wagner, R. Zur vergleichenden Physiologie des Blutes, Untersuchungen über Blutkörperchen, Blutbildung, und Blutbahn, nebst Bemerkungen über Blutbewegung, Ernährung und Absonderung. Leopold Voss.; Leipzig: 1833.

204. Wagner, R. Icones physiologicae. Erläuterungstafeln zur Physiologie und Entwicklungsgeschichte. Leopold Voss; Leipzig: 1839.

205. Walcheck B, Moore KL, McEver RP, Kishimoto TK. Neutrophil-neutrophil interactions under hydrodynamic shear stress involve L-selectin and PSGL-1. J. Clin. Invest. 1996; 98:1081–1087. [PubMed: 8787668]

206. Waldron TT, Springer TA. Transmission of allostery through the lectin domain in selectin-mediated cell adhesion. Proc. Natl. Acad. Sci. USA. 2009; 106:85–90. [PubMed: 19118202]

207. Waller A. Microscopic examination of some principal tissues of the animal frame as observed in the tongue of the living frog, toad, etc. London, Edinburgh and Dublin Philos. Mag. 1846; 29:271–287.

208. Waugh, RE. Membrane tethers, chapter 1. In: Ley, K., editor. Leukocyte adhesion. Vol. 64. Academic press; San Diego: 2009. p. 3-24.

209. Waugh RE, Bauserman RG. Physical measurement of bilayer-skeletal separation forces. Ann. Biomed. Eng. 1995; 23:308–321. [PubMed: 7631984]

210. Waugh RE, Hochmuth RM. Mechanical equilibrium of thick, hollow, liquid membrane cylinders. Biophys. J. 1987; 52:391–400. [PubMed: 3651558]

211. Weller A, Isenmann S, Vestweber D. Cloning of the mouse endothelial selectins. Expression of both E- and P-selectin is inducible by tumor necrosis factor alpha. J. Biol. Chem. 1992; 267:15176–15183. [PubMed: 1378846]

212. Wild MK, Huang M-C, Schulze-Horsel U, et al. Affinity, kinetics, and thermodynamics of E-selectin binding to E-selectin ligand-1. J. Biol. Chem. 2001; 276:31602–31612. [PubMed: 11404363]

213. Xia L, Ramachandran V, McDaniel JM, et al. N-terminal residues in murine P-selectin glycoprotein ligand-1 required for binding to murine P-selectin. Blood. 2003; 101:552–559. [PubMed: 12393631]

214. Xia L, Sperandio M, Yago T, McDaniel JM, et al. P-selectin glycoprotein ligand-1-deficient mice have impaired leukocyte tethering to E-selectin under flow. J. Clin. Invest. 2002; 109:939–950. [PubMed: 11927621]

215. Xu G, Shao J-Y. Double tether extraction from human neutrophils and Its comparison with CD4+ T-lymphocytes. Biophys. J. 2005; 88:661–669. [PubMed: 15475589]

216. Xu G, Shao JY. Human neutrophil surface protrusion under a point load: location independence and viscoelasticity. Am. J. Physiol. Cell Physiol. 2008; 295:C1434–C1444. [PubMed: 18815230]

217. Yago T, Fu J, McDaniel JM, et al. Core 1-derived O-glycans are essential E-selectin ligands on neutrophils. Proc. Natl. Acad. Sci. USA. 2010; 107:9204–9209. [PubMed: 20439727]

218. Yago T, Leppanen A, Qiu H, Marcus WD, Nollert MU, Zhu C, Cummings RD, McEver RP. Distinct molecular and cellular contributions to stabilizing selectin-mediated rolling under flow. J. Cell Biol. 2002; 158:787–799. [PubMed: 12177042]

219. Yago T, Wu J, Wey CD, Klopocki AG, Zhu C, McEver RP. Catch bonds govern adhesion through L-selectin at threshold shear. J. Cell Biol. 2004; 166:913–923. [PubMed: 15364963]

220. Yago T, Zarnitsyna VI, Klopocki AG, McEver RP, Zhu C. Transport governs flow-enhanced cell tethering through L-selectin at threshold shear. Biophys. J. 2007; 92:330–342. [PubMed: 17028146]

221. Yu Y, Shao JY. Simultaneous tether extraction contributes to neutrophil rolling stabilization: a model study. Biophys. J. 2007; 92:418–429. [PubMed: 17071668]

222. Zarbock A, Abram CL, Hundt M, Altman A, Lowell CA, Ley K. PSGL-1 engagement by E-selectin signals through Src kinase Fgr and ITAM adapters DAP12 and FcR gamma to induce slow leukocyte rolling. J. Exp. Med. 2008; 205:2339–2347. [PubMed: 18794338]

223. Zarbock A, Lowell CA, Ley K. Spleen tyrosine kinase Syk is necessary for E-selectin-induced alpha(L)beta(2) integrin-mediated rolling on intercellular adhesion molecule-1. Immunity. 2007; 26:773–783. [PubMed: 17543554]

224. Zarbock A, Muller H, Kuwano Y, Ley K. PSGL-1-dependent myeloid leukocyte activation. J. Leukoc. Biol. 2009

225. Zarbock A, Singbartl K, Ley K. Complete reversal of acid-induced acute lung injury by blocking of platelet-neutrophil aggregation. J. Clin. Invest. 2006; 116:3211–3219. [PubMed: 17143330]

226. Zhao Y, Chien S, Skalak R. A stochastic model of leukocyte rolling. Biophys. J. 1995; 69:1309–1320. [PubMed: 8534801]

227. Zhu C, Long M, Chesla SE, Bongrand P. Measuring receptor/ligand interaction at the single-bond level: experimental and interpretative issues. Ann. Biomed. Eng. 2002; 30:305–314. [PubMed: 12051616]

228. Zhu C, Yago T, Lou J, et al. Mechanisms for flow-enhanced cell adhesion. Ann. Biomed. Eng. 2008; 36:604–621. [PubMed: 18299992]

229. Cao J, Donell B, Deaver DR, Lawrence MB, Dong C. In vitro side-view imaging technique and analysis of human T-leukemic cell adhesion to ICAM-1 in shear flow. Microvasc Res. 1998; 55:124–137. [PubMed: 9521887]

230. Pospieszalska, MK.; Lasiecka, I.; Ley, K. Cell protrusions and tethers: a unified approach. submitted to *Biophysical Journal*

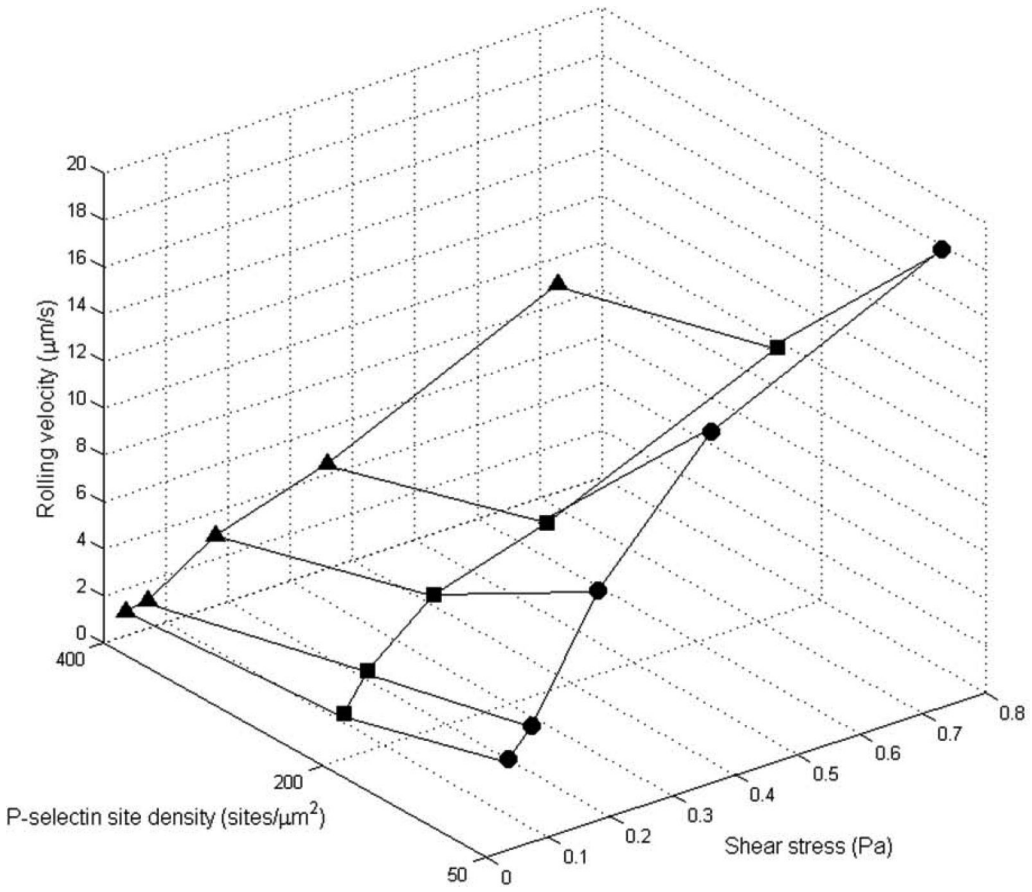

Fig. 1.

In vitro rolling velocity of human neutrophils plotted as a function of P-selectin site density and wall shear stress. Data reproduced from Ref. [105]. Closed triangle (400 sites/μm^2), closed square (200 sites/μm^2), and closed circle (50 sites/ μm^2).

Fig. 2.

Forces acting on a rolling neutrophil. F_s and T_s are the shear force (along *x*-axis) and torque (along *y*-axis about the cell center), respectively, exerted by the streaming fluid on the rolling cell. A single long tether 'te1' (representative of n tethers) and a stressed microvilli 'mv1' (representative of m stressed tetherless microvilli) are shown. The distance of the tether and microvillus bonds anchorage points from the center of the cell is denoted as L_i (i = 1 to n) and l_j (j = 1 to m), respectively. The tethers and the stressed microvilli are shown to form an angle φ_i (i = 1 to n) and θ_j (j = 1 to m) with the P-selectin substrate, respectively. The hydrodynamic force acting on the tethers and stressed tetherless microvilli is denoted as $F_{te,i}$ (i = 1 to n) and $F_{mv,j}$ (j = 1 to m), respectively. The cell radius is denoted by r_c. The normal reaction force exerted by the substrate on the cell is denoted as F_N. P-selectin on the substrate and PSGL-1 on the microvilli shown in blue and green color, respectively. The Cartesian coordinate system is shown in grey. $v_x(z)$ is the fluid velocity along *x*-axis. Not drawn to scale. Symbols of biophysical parameters are also explained in Table 2.

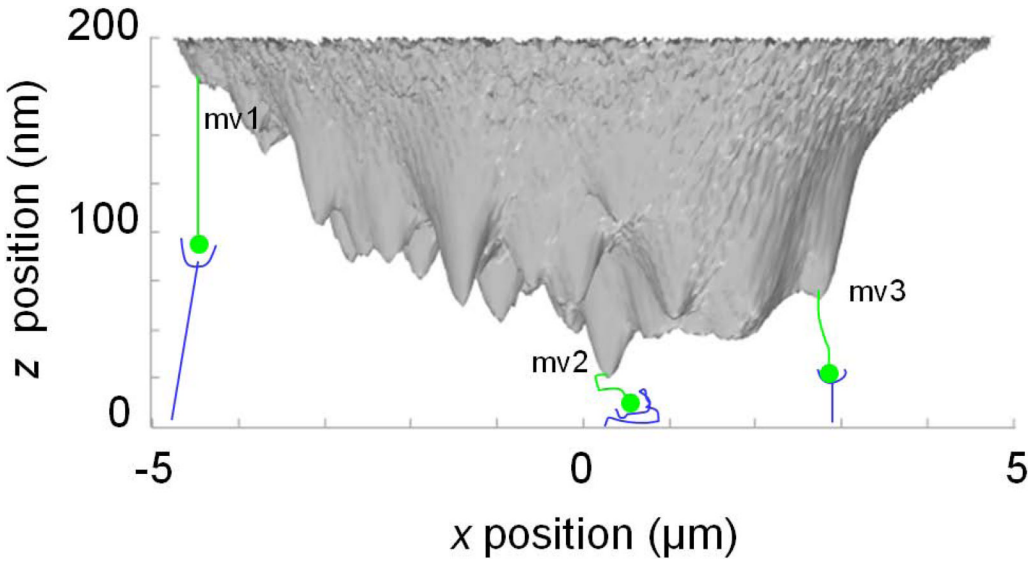

Fig. 3.

Stressed, compressed, and unstressed bonds in the footprint of a rolling neutrophil [3D-reconstruction adapted from Sundd, P. *et al. Nat Methods* **7**, 821-824 (2010) with permission]. 3D reconstruction of the footprint of an EGFP-expressing neutrophil rolling on P-selectin coated substrate generated using qDF microscopy. A microvillus is defined as a conical protrusion longer than 25 nm in *z*-direction. Only three microvilli (mv1, mv2, and mv3) are labeled. Schematics of P-selectin-PSGL-1 molecular complex (not to scale) drawn on the tips of microvilli. As the cell rolls from left to right, the P-selectin-PSGL-1 bonds are formed in the front at the unstressed length (L_{sep} ~ 70 nm; mv3), compressed in the center (L_{sep} < 70 nm; mv2) and stressed beyond the unstressed length (L_{sep} > 70 nm; mv3) at the rear of the footprint where they finally break. P-selectin and PSGL-1 shown as blue and green, respectively. Wall shear stress 0.6 Pa. P-selectin 20 molecules/μm^2.

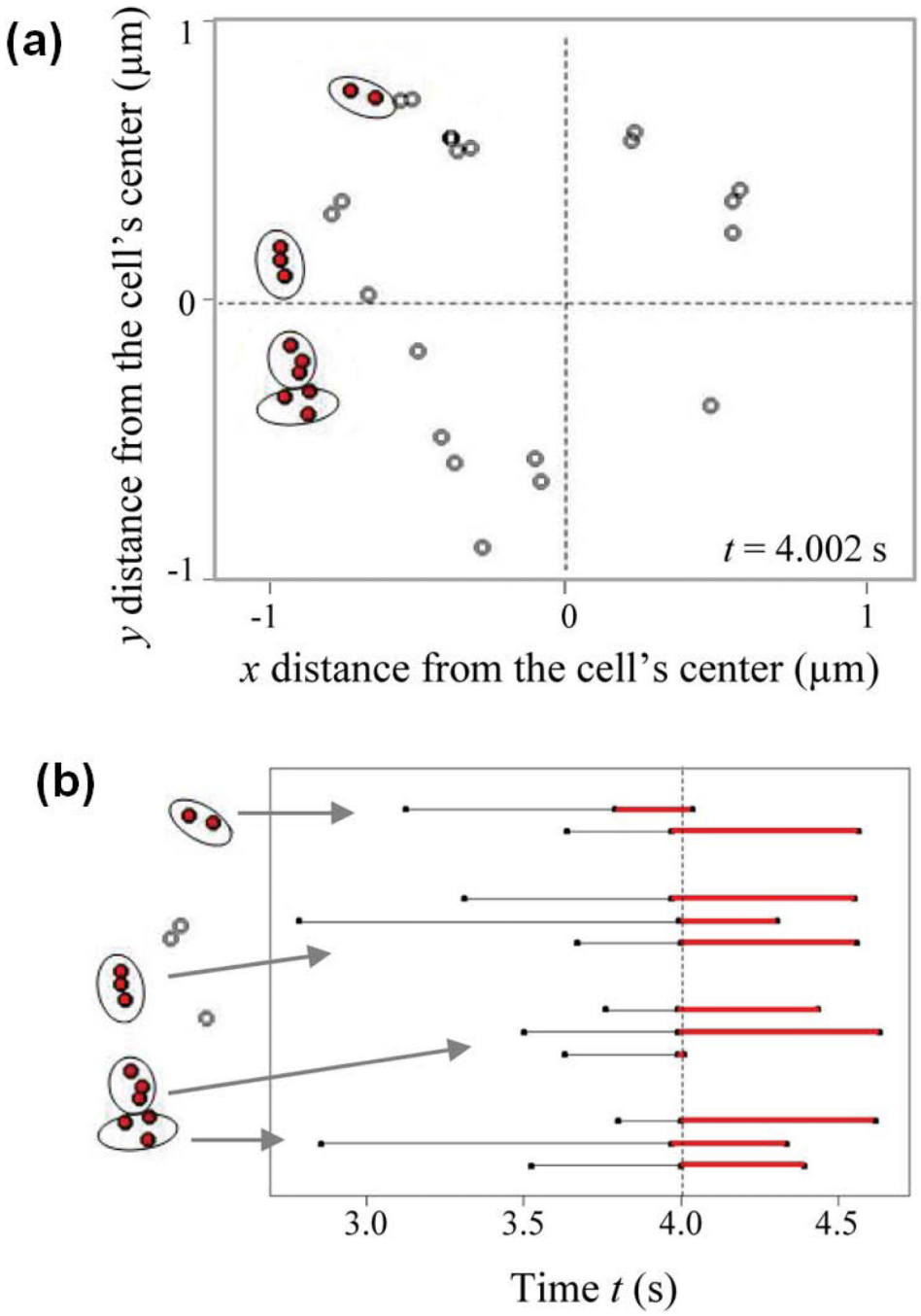

Fig. 4.

ETMA simulations reveal bond clusters in the footprint of a rolling neutrophil. (a) Distribution of the PSGL-1-P-selectin bond bases in the footprint of a rolling neutrophil (the cell translates in the positive *x*-direction). The load-bearing bonds are marked with red circles. Ovals indicate the load-bearing bond clusters and each cluster corresponds to a different microvillus. (b) Lifetime of 11 load-bearing bonds seen in (a). Each bond is represented by a black segment (the no-load time period) and a red segment (the load time period). All bonds but one become load-bearing at the same time (t = 4 s). Unpublished data (Pospieszalska and Ley).

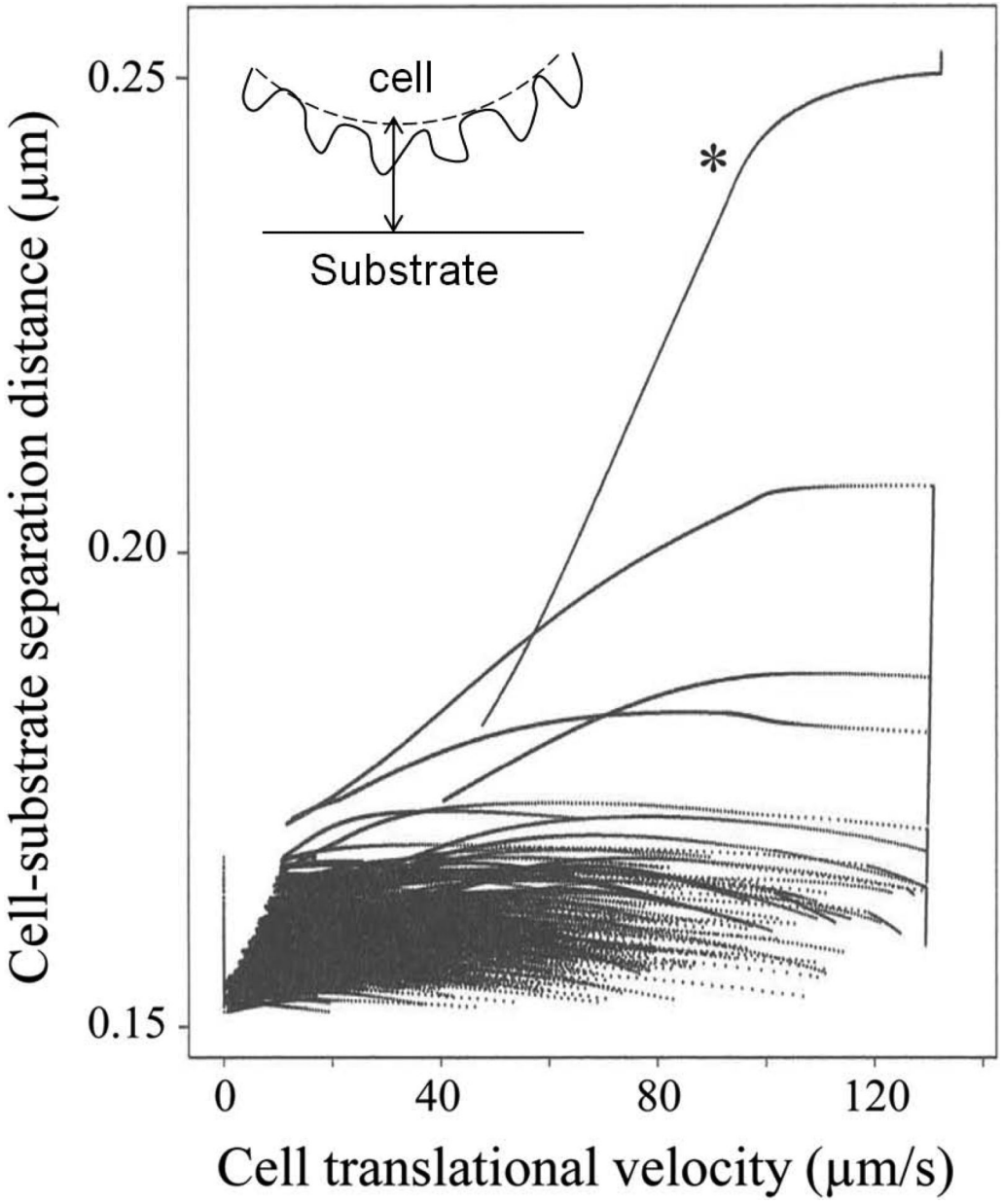

Fig. 5.

Scatter plot showing cell translational velocity as a function of cell body to substrate seperation distance (distance does not include microvilli-see inset). Instantaneous changes in the separation distance are seen as individual traces. The asterisk indicates the trace representing the first approach of the cell to the substrate. The almost vertical trace for the high translational velocities represents instantaneous changes in the separation distance when no load-bearing bonds were present. The trace discontinuity near velocity zero is due to a discrete process of modeling owing to the time step. Unpublished data (Pospieszalska and Ley).

Fig. 6.

Whole cell deformation results in a larger footprint at high shear stress [(b) and (c) adapted from Sundd, P. *et al. Nat Methods* **7**, 821-824 (2010) with permission]. (a) A schematic showing the side and bottom views of the footprint of a rolling neutrophil following deformation by the shear forces to a nonspherical shape. Dashed circle shows the nondeformed neutrophil for comparison. Red closed circles are the tips of microvilli in the footprint. (b) Coordinates of the microvilli tips in the footprint of an EGFP-expressing neutrophil rolling on P-selectin substrate extracted from qDF micrographs. P-selectin 20 molecules/μm^2. Wall shear stress 0.6 Pa. (c) Coordinates of the microvilli tips in the footprint of a non-deformable spherical rolling neutrophil revealed using ETMA simulations. P-selectin 150 molecules/μm^2. Wall shear stress 0.05 Pa. Color of the data points in (b) and (c) represents the *z*-coordinates of microvilli tips based on color bars shown on the right. Black arrows denote the direction of rolling.

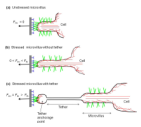

Fig. 7.

Microvillus deformation under tensile force. Schematic showing a neutrophil interacting with a P-selectin coated substrate through PSGL-1 expressed on the microvillus tip. To denote the individual microvillus/tether force acting on the cell, symbol F_{mv} is used when there is no tether and symbol F_{te} when a tether is present. (a) Unstressed microvillus for $F_{mv} = 0$. (b) Stressed microvillus without tether for $0 < F_{mv} < F_{th}$. (c) Stressed microvillus with a long membrane tether formed following dissociation of plasma membrane from the cytoskeleton under force $F_{te} = F_{mv} > F_{th}$. The symbols for biophysical parameters are defined in Table 2. P-selectin and PSGL-1 shown as blue and green, respectively. Actin cytoskeleton shown in red. Tether anchorage point shown as a round structure at the end of tether. Not drawn to scale.

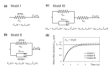

Fig. 8.

Models for the microvillus extension material used in published PSGL-1/P-selectin pulling experiments. (a) Elastic model represented by a spring. (b) Kelvin-Voigt viscoelastic model represented by a spring and a dashpot connected in parallel. (c) Viscoelastic model composed of a Kelvin-Voigt unit and an elastic unit connected in series. In a-c, σ_{mv} and κ_{mv} are the spring constants for the corresponding springs, η_{eff_mv} is the effective viscosity of the dashpot, F_{mv} is the pulling force, L_{mv} is the microvillus extension, $\dot{L}_{mv} = dL_{mv}/dt$ is the microvillus extension rate, and $\dot{F}_{mv} = dF_{mv}/dt$ is the loading rate. (d) Microvillus extension under a constant force, F_{mv} = 45 pN, described by the models a-c for σ_{mv} = 43 pN/μm, = η_{eff_mv} = 33 pN s/μm, and κ_{mv} = 800 pN/μm.

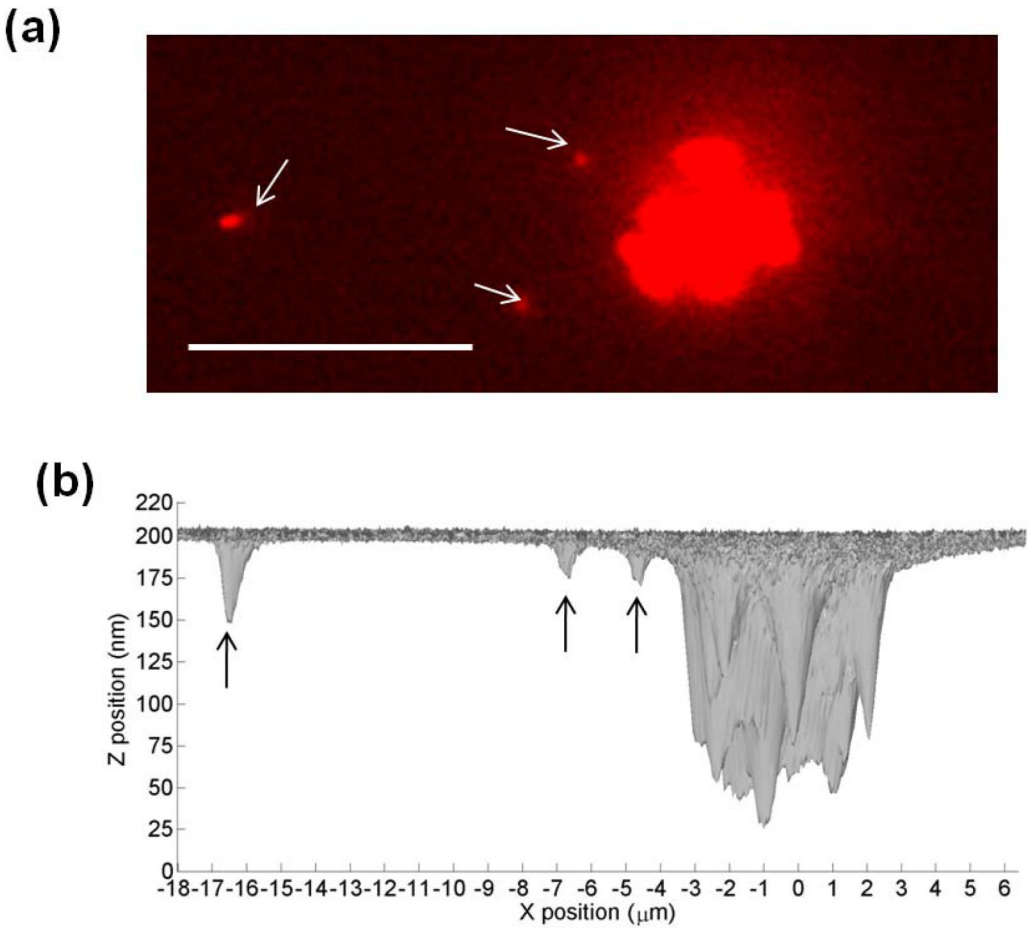

Fig. 9.

Long tethers facilitate neutrophil rolling at high shear stress [Adapted from Sundd, P. *et al. Nat Methods* **7**, 821-824 (2010) with permission]. (a) qDF micrograph of a DiI-labeled neutrophil rolling on P-selectin substrate processed to saturation to reveal anchorage points of long tethers behind the footprint. (b) 3D reconstruction of the footprint shown in (a) reveals *z* position of tether anchorage points above the P-selectin substrate which is equal to the length of the stressed P-selectin-PSGL-1 bonds holding the tether anchorage point to the substrate. P-selectin 20 molecules/μm^2. Wall shear stress 0.8 Pa. Flow is from left to right. Scale bar 10 μm. Arrows mark tether anchorage points.

Table 1

Adhesion receptors mediating neutrophil rolling and tethering *in vivo* and *in vitro*.

Receptor	Extracellular length (nm)	Expression	Molecular Density	Role in leukocyte recruitment	Physiological ligand
Hu P-selectin	38	Inducible	20-50 molecules/μm^2 on cultured HUVEC	Tethering and rolling	PSGL-1 on neutrophils, monocytes, and Th1 cells*
Mu P-selectin	34	Inducible	No data	Tethering and rolling	PSGL-1 on neutrophils, monocytes and Th1 cells*
Hu E-selectin	27	Inducible	750 molecules/μm^2 on cultured HMVEC	Slow rolling	PSGL-1, sialylated glycosphingolipids, and sLe^x bearing glycoproteins on neutrophils
Mu E-selectin	27	Inducible	No data	Slow rolling	PSGL-1, ESL-1, CD44, and core O-derived glycans bearing glycoproteins on neutrophils
Hu L-selectin	12	Constitutive	Neutrophils (30,000-40,000 molecules), monocytes, lymphocytes	Tethering, secondary capture, and rolling (only in HEVs)	PSGL-1 on neutrophils and monocytes, PNAds (GlyCAM-1, CD34, and podocalyxin) on EC in HEVs of lymph nodes
Mu L-selectin	12	Constitutive	Neutrophils, monocytes, lymphocytes	Tethering, secondary capture, and rolling (only in HEVs)	PSGL-1 on neutrophils and monocytes, PNAds (GlyCAM-1, CD34, and podocalyxin) on EC in HEVs of lymph nodes
Hu PSGL-1	50	Constitutive	Neutrophils (18,000-25,000 molecules), monocytes, Th1 cells*	Tethering, rolling, and secondary capture	P- and E-selectin on EC and L-selectin on neutrophils, and monocytes
Mu PSGL-1	50	Constitutive	Neutrophils (75,000 molecules), monocytes, Th1 cells*	Tethering, rolling, and secondary capture	P- and E-selectin on EC and L-selectin on neutrophils, and monocytes

Hu, human; Mu, murine; HUVEC, human umblical-cord vascular endothelial cells; HMVEC, human micro-vascular endothelial cells; HEVs, high endothelial venules; PSGL-1, P-selectin glycoprotein ligand-1; ESL-1, E-selectin ligand-1; sLe^x, sialyl Lewis x; EC, endothelial cells.

*PSGL-1 is expressed on other leukocytes, but is correctly glycosylated only on myeloid cells and Th1 cells.

Table 2

Nomenclature of biophysical parameters.

Symbol	Parameter
F_s	Hydrodynamic shear force acting on rolling neutrophil along *x*-axis (pN)
T_s	Hydrodynamic torque acting on rolling neutrophil (about the cell center) along *y*-axis (pN.μm)
F_N	Normal reaction force acting on rolling neutrophil (pN)
r_c	Cell radius (μm)
τ_w	Wall shear stress (Pa)
$v_x(z)$	*x*-component of fluid velocity as a function of *z* distance from the substrate
$F_{te,i}$	Force on i^{th} tether (pN)
$F_{mv,j}$	Force on j^{th} stressed tetherless microvillus (pN)
φ_i	Tether angle with the P-selectin substrate (degrees)
θ_j	Angle of stressed tetherless microvillus with P-selectin substrate (degrees)
$T_{te,i}$	Torque (about the cell center) acting on rolling neutrophil along *y*-axis due to the tether force $F_{te,i}$ (pN μm)
$T_{mv,j}$	Torque (about the cell center) acting on rolling neutrophil along *y*-axis due to the microvillus force $F_{mv,j}$ (pN μm)
L_i	Distance (along *x*-axis) of the anchorage point of tether bonds from the center of the cell (μm)
l_j	Distance (along *x*-axis) of the anchorage point of stressed (tetherless) microvillus bonds from the center of the cell (μm)
F_b	Bond force (pN)
σ	Bound state spring constant of the bond (pN/μm)
L_{sep}	Stressed length of the bond (nm)
λ	Unstressed length of the bond (nm)
R	Receptor
L	Ligand
RL	Receptor-ligand complex
k_f^o	Unstressed forward reaction rate at $F_b = 0$ ($M^{-1}s^{-1}$)
k_r^o	Unstressed reverse reaction rate at $F_b = 0$ (s^{-1})
k_f	Forward reaction rate at $F_b > 0$ ($M^{-1}s^{-1}$)
k_r	Reverse reaction rate at $F_b > 0$ (s^{-1})
γ	Reactive compliance (Å)
κ_B	Boltzmann's constant (J/°K)
T	Absolute temperature (°K)
L_{new}	Length of the possible new bond (nm)
σ_{ts}	Transition state spring constant (pN/μm)
k_{1rup}	Reverse reaction rate for pathway 1 (s^{-1})
k_{2rup}	Reverse reaction rate for pathway 2 (s^{-1})
k_2^o	Unstressed reverse reaction rate for the pathway 2 at $F_b = 0$ (s^{-1})
S_1/S_2	Occupancy ratio of the two bound states
Φ_o	Occupancy ratio of the two bound states at $F_b = 0$

Symbol	Parameter
f_{12}	Bond force at which occupancy ratio changes 2.7 fold (pN)
ΔE_{21}	Energy barrier between two bound states (J)
$F_{mv}(t)$	Pulling force on the microvillus (pN)
$\dot{F}_{mv}(t)$	Loading rate (pN/s) for microvillus
F_{th}	Threshold force for dissociation of membrane from cytoskeleton (pN)
$L_{mv}(t)$	Microvillus extension (μm)
$\dot{L}_{mv}(t)$	Rate of microvillus extension (μm/s)
σ_{mv}	Microvillus spring constant (pN/ μm)
κ_{mv}	Spring constant of the second elastic unit in Fig. 8(c) (pN/ μm)
η_{eff_mv}	Effective viscosity of microvilli (pN s/ μm)
$F_{te}(t)$	Pulling force on tether (pN)
$\dot{F}_{te}(t)$	Loading rate (pN/s) for tether
$L_{te}(t)$	Tether extension (μm)
$\dot{L}_{te}(t)$	Rate of tether extension (μm/s)
η_{eff_te}	Effective viscosity of tether (pN s/ μm)
k_c	Cell membrane curvature modulus (pN μm)
d_{int}	Interfacial drag coefficient (pN s/μm^3)

Symbols for different biophysical parameters are defined. Units are shown in parenthesis.

Table 3

Kinetic parameters for different receptor-ligand pairs.

Receptor-ligand	$k_f^o(\mathrm{M^{-1}s^{-1}})$	$k_r^o(\mathrm{s^{-1}})$	K_d (μM)	γ (Å)	Ref.
P-selectin-PSGL-1	4.4×10^6	1.4	0.3		[130]
P-selectin-PSGL-1	-	1	-	0.5	[7]
P-selectin-PSGL-1	-	0.95	-	0.39	[5]
P-selectin-PSGL-1	9.3×10^5	1.4	1.5	-	[90]
P-selectin-PSGL-1	-	2.68	-	-	[29]
P-selectin-PSGL-1	-	0.55	-	-	[227]
P-selectin-PSGL-1	-	0.9	-	-	[70]
P-selectin-PSGL-1	-	0.84	-	0.68	[27]
P-selectin-PSGL-1	-	0.19	-	1.2	[61]
P-selectin-PSGL-1	-	0.18	-	1.35	[62]
sP-selectin-PSGL-1	-	1.1	-	0.7	[156]
mdP-selectin-PSGL-1	-	1	-	0.42	[156]
L-selectin-PSGL-1	-	10.2	47	-	[29, 90]
L-selectin-PSGL-1	-	7	-	0.24	[4]
L-selectin-PSGL-1	-	0.83	-	1.51	[62]
L-selectin-PNAd	-	6.6	-	0.19	[5]
L-selectin-GlyCAM-1	$\geq 10^5$	≥ 10	108	-	[135]
E-selectin-PSGL-1	-	0.24	-	1.11	[62]
E-selectin-ESL-1	7.4×10^4	4.6	62	-	[212]
E-selectin-ESL	-	0.7	-	0.3	[5]
E-selectin-sLe^x	-	0.82	-	0.34	[195]

For the different ligand pairs, k_f^o – unstressed forward reaction rate, k_r^o – unstressed reverse reaction rate, K_d – equilibrium dissociation constant, and γ – reactive compliance were estimated by different studies mentioned under Ref. sP-selectin, soluble monomeric P-selectin, mdP-selectin, membrane dimeric P-selectin and ESL, an E-selectin ligand on human neutrophil.